Materials Today Bio 32 (2025) 101763

Contents lists available at ScienceDirect

Materials Today Bio

journal homepage: www.journals.elsevier.com/materials-today-bio

Recent advances in fluorescent nanomaterials designed for biomarker detection and imaging

Xuming Sun [a,b,*], Tong Xiang [a,b], Linyan Xie [c,**], Qiongqiong Ren [a,b], Jinlong Chang [a], Wenshuai Jiang [a,b], Zhen Jin [a,b], Xiuli Yang [d], Wu Ren [a,***], Yi Yu [a,****]

[a] School of Medical Engineering, Xinxiang Medical University, Xinxiang, 453003, PR China
[b] Xinxiang Key Laboratory of Neurobiosensor, Xinxiang Medical University, Xinxiang, 453003, PR China
[c] School of Mathematical Medicine, Xinxiang Medical University, Xinxiang, 453003, PR China
[d] Department of Cardiology, The Third Affiliated Hospital of Xinxiang Medical University, Xinxiang, 453003, PR China

ARTICLE INFO

Keywords:
Biomarker
Fluorescence
Nanomaterials
Imaging

ABSTRACT

The highly sensitive detection and imaging of biomarkers are critical for early diagnosis, treatment, and prognosis monitoring. The unique size and structure of fluorescent nanomaterials provide key benefits such as excellent photostability, high fluorescence quantum yield, and tunable excitation and emission wavelengths. These properties have led to the widespread application of nanomaterials in fluorescent biomarkers detection and imaging. In this review, we began by introducing the composition of fluorescent probes and discussing the underlying sensing mechanisms. We then summarized recent advances in the use of fluorescent nanomaterials such as quantum dots (QDs), metal nanoclusters (MNCs), carbon dots (CDs), and metal-organic frameworks (MOFs) for biomarker detection and imaging. Additionally, we highlighted the applications of fluorescent nanomaterials in the detection and imaging of small molecules, biomacromolecules, and various biomarkers, including metal ions, bacteria, and circulating tumor cells (CTCs). The challenges and future prospects of fluorescent nanomaterials in biomarker detection and imaging were also discussed. We anticipate that fluorescent nanomaterials will have profound implications for clinical biomarker detection and imaging, with considerable application in both academic research and industrial applications.

1. Introduction

During the course of disease progression, disturbances in biological systems can lead to the abnormal expression of active substances within the organism. Biomarkers are biological molecules that undergo specific biochemical changes during disease development [1]. They are typically classified into small molecules, large molecules (e.g., proteins, nucleic acids), and other markers based on their composition [2,3]. Given that biomarkers reflect the interactions between biological systems and underlying pathological states, it is crucial to establish accurate, sensitive, and convenient biomarker detection technologies for early disease diagnosis and health monitoring [4,5]. However, current methods for detecting biomarkers such as computed tomography (CT), and mass spectrometry imaging (MSI) still face various of challenges, including complex processes, high cost, cumbersome procedures, and insufficient sensitivity, which limit their ability to accurately analyze trace biomarkers. Therefore, developing high-sensitivity and high-accuracy detection strategies to enable efficient analysis of trace biomarkers is an urgent task.

Biosensing technologies have been widely used for the highly sensitive detection of biomarkers due to their good selectivity, high sensitivity, rapid response, low cost, and ability to perform continuous online monitoring [6–8]. Notably, fluorescence detection technology has emerged as one of the most promising techniques in biomarker detection, offering advantages such as high sensitivity, high spatial resolution, and dynamic biomarker monitoring [9–11]. Fluorescent probes can

This article is part of a special issue entitled: Biomarker published in Materials Today Bio.

* Corresponding author. School of Medical Engineering, Xinxiang Medical University, Xinxiang, 453003, PR China.
** Corresponding author.
*** Corresponding author.
**** Corresponding author.
E-mail addresses: sunxuming@xxmu.edu.cn (X. Sun), jielinyan@163.com (L. Xie), renwu88@126.com (W. Ren), yuyi@xxmu.edu.cn (Y. Yu).

https://doi.org/10.1016/j.mtbio.2025.101763
Received 24 January 2025; Received in revised form 9 April 2025; Accepted 11 April 2025
Available online 12 April 2025

specifically bind to biomarkers and be detected by the excitation and emission of fluorescent signals. This process provides not only quantitative information but also enables real-time monitoring of the distribution and dynamic changes of biomarkers within cells or tissues [12,13]. When integrated with super-resolution microscopy techniques such as stimulated emission depletion microscopy (STED), structured illumination microscopy (SIM), and single-molecule localization microscopy (SMLM), fluorescence detection technology enables imaging at the nanoscale, offering significant potential for tracking dynamic cellular events, visualizing biomolecular interactions, and detecting biomarkers at the molecular level [14]. As the range of available fluorescent probes continues to expand, fluorescence detection technology is evolving from single-molecule detection to complex multiplexed biomarker detection, thereby enhancing its applicability in early disease screening, prognosis assessment, and drug development. However, existing fluorescent probes still encounter technical challenges, such as poor photostability, inadequate specificity, and limited detection depth. Therefore, the development of new, higher-performance fluorescent probes is critical to advancing biomarkers detection and imaging.

Nanomaterial probes have become an essential component of fluorescence detection technology due to their unique optical properties and favorable biocompatibility in recent years [15,16]. By manipulating parameters such as morphology, size, and surface modification, nanomaterials can be optimized to enhance their fluorescence properties, improving their performance in biomarker detection [17,18]. The utilization of nanomaterials, including quantum dots (QDs) [19], metal nanoclusters (MNCs) [20], carbon dots (CDs) [21], and metal-organic frameworks (MOFs) [22], has been demonstrated to exhibit superior photostability and fluorescence intensity. Moreover, surface modification or functionalization enables highly selective recognition of specific biomarkers. [23]. The incorporation of nanomaterials in fluorescence imaging improves detection sensitivity and expands the range of in vivo imaging applications, showcasing substantial potential for early diagnosis and clinical treatment monitoring. Compared with the previous reviews, this work provided a comprehensive overview of nanomaterial-based probes, covering detection mechanisms, types of nanomaterials, and practical applications, as shown in Scheme 1. In addition, the potential applications of machine learning in this field were discussed, providing a broader perspective on the future development of fluorescent nanomaterials for biomarker detection and imaging.

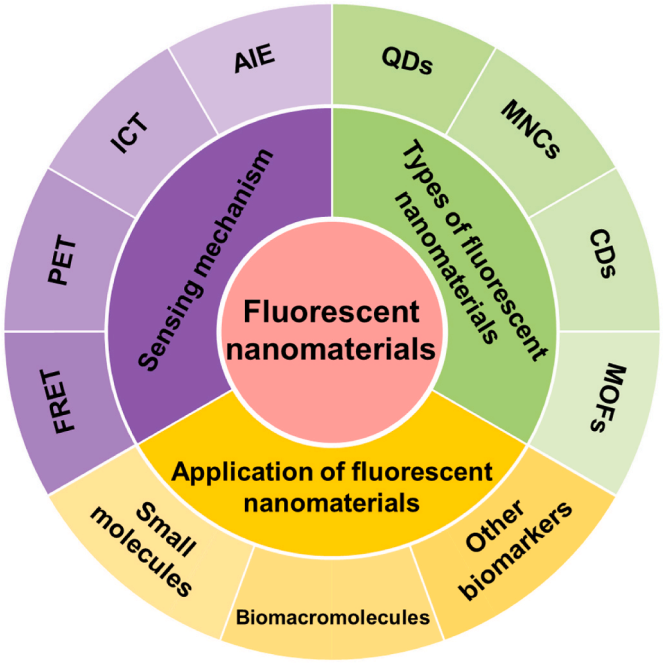

Scheme 1. Scheme of fluorescent nanomaterials designed for biomarker detection and imaging, including sensing mechanism, types of fluorescent nanomaterials and the application in biomarker detection.

In conclusion, the continued development of nanotechnology and fluorescent probe technology holds great promise for the application of biomarker detection and imaging. This review first introduced the composition and mechanisms of fluorescent probes, followed by a summary of the use of fluorescent nanomaterials, including QDs, MNCs, CDs, and MOFs, in biomarker detection and imaging. It then highlighted recent advances in the use of fluorescent nanomaterials for the detection and imaging of small molecules, biomolecules, and other biomarkers (such as metal ions, bacteria, and circulating tumor cells). Finally, the challenges and future prospects of fluorescent nanomaterials in biomarker detection and imaging were discussed. We hope this review will contribute to the design of novel, highly sensitive fluorescent nanomaterials and promote their application in clinical biomarker detection and imaging.

2. Fluorescence detection background and theory

2.1. Composition of fluorescent probes

Fluorescence is a distinct photoluminescence phenomenon in which fluorescent molecules absorb excitation light and transition from the ground state to an excited state. The inherent instability of the excited state results in a rapid return to the ground state, releasing energy in the form of light and heat [15]. In fluorescence-based biomarker detection and imaging, fluorescent probes play a pivotal role by simultaneously recognizing target analytes and generating fluorescent signals [24,25]. The design and material composition of these probes significantly influence key detection attributes such as signal sensitivity, stability, and overall performance.

Fluorescent probes typically consist of three key components: the recognition unit (receptor), the fluorescence unit (fluorophore), and the connector/linker (spacer) [26]. The recognition unit is specifically designed to bind to the target analyte, enabling selective interaction with the substance of interest. This selective binding is critical for the probe's ability to detect and quantify the target analyte, necessitating the use of tailored recognition units and methods for different test substances. The connector, which acts as a molecular recognition hub, links the recognition unit and the fluorophore. The fluorophore emits the fluorescent signal that serves as the readout of the detection system. The sensitivity of fluorescent probes is predominantly determined by the fluorophore, whose structural design and material selection play a critical role in influencing the detection performance. The early fluorescent materials used for biomarker detection and imaging were mainly organic small molecules (OFMs), while inorganic fluorescent nanomaterials have unique optical and chemical properties, such as bright photoluminescence, good photostability, and good biocompatibility, and have been widely used in the structural design of fluorescent probes.

2.2. Sensing mechanism of fluorescent probes

The mechanism of fluorescent probe interaction with target biomarkers is fundamental to constructing efficient probes and achieving sensitive detection. Current design and detection mechanisms for fluorescent probes include fluorescence resonance energy transfer (FRET), photoinduced electron transfer (PET), intramolecular charge transfer (ICT), and aggregation-induced luminescence (AIE) (Fig. 1).

2.2.1. Fluorescence resonance energy transfer (FRET)

FRET involves the distance-dependent transfer of energy between two light-sensitive molecules (donor and acceptor) (Fig. 1A). Upon excitation by light at a specific wavelength, one fluorophore acts as an energy donor, transferring excitation energy to a nearby acceptor via

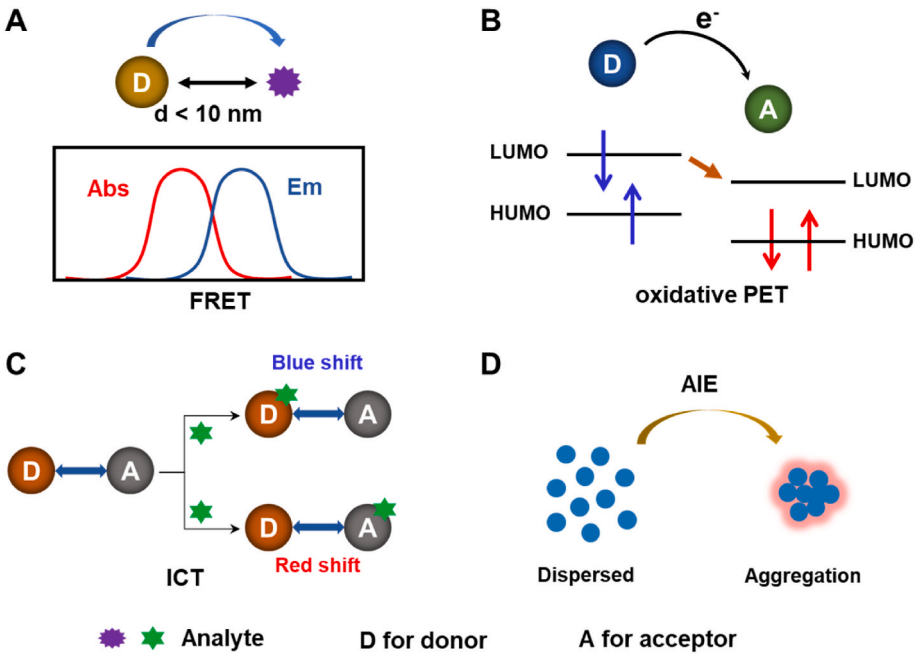

Fig. 1. Scheme of four common fluorescence biosensing mechanisms. (A) Schematic illustration of fluorescence resonance energy transfer (FRET), (B) Schematic illustration of photoinduced electron transfer (PET), (C) Schematic illustration of intramolecular charge transfer (ICT), and (D) Schematic illustration of aggregation-induced luminescence (AIE).

dipole-dipole interactions [27]. This process requires spectral overlap between the donor's fluorescence emission and the acceptor's excitation wavelength. The efficiency of energy transfer is highly dependent on the donor-acceptor distance, governed by an inverse sixth-power relationship, with optimal spacing generally under 10 nm [28].

FRET-based fluorescent probes are widely used in fluorescent sensing, enhancing detection sensitivity and efficiency [28,29]. In designing FRET-based probes, various strategies are employed: (i) the target analyte reacts with the acceptor, quenching its fluorescence and altering donor-acceptor energy transfer, thereby modifying the system's luminescence; (ii) target binding to the acceptor induces spatial site-blocking, increasing donor-acceptor distance, which diminishes FRET efficiency and alters fluorescence; (iii) strong target binding to the acceptor disrupts the donor-acceptor connection, restoring donor fluorescence; and (iv) the target acts as the energy acceptor, directly interacting with the donor to construct a FRET system, leading to reduced donor fluorescence intensity. Consequently, FRET-based fluorescent probes necessitate precise design and characterization of optical properties and structural parameters of the fluorescent materials.

2.2.2. *Photoinduced electron transfer (PET)*

PET is a widely utilized mechanism in fluorescent chemical sensors (Fig. 1B). PET-based systems typically also consist of three key components: the florescent probes (donor), the analyte (acceptor), and a connecting structure [20]. PET can occur in two distinct forms: reducing PET and oxidative PET. In reducing PET, fluorescent nanomaterials function as electron acceptors, with electrons transferring from the recognizer's highest occupied molecular orbital (HOMO) to the acceptor's HOMO. In contrast, in oxidative PET, fluorescent nanomaterials act as electron donors, with electrons transferring from the donor's lowest unoccupied molecular orbital (LUMO) to the acceptor's LUMO [23]. This mechanism allows for sensitive and dynamic control of fluorescence intensity in response to environmental changes or the presence of target analytes.

In PET-based probes, fluorescence is restored upon target binding, which restricts electron transfer between the luminescent material and the acceptor. These probes are particularly suited for detecting metal ions, leveraging elements with lone electron pairs (e.g., oxygen and nitrogen) for strong coordination interactions with metal ions.

2.2.3. *Intramolecular charge transfer (ICT)*

ICT plays a crucial role in numerous physical and biological systems and is extensively used in signal modulation for fluorescent probes (Fig. 1C). ICT-based probes typically include an electron donor and an electron acceptor to form a donor-π-acceptor system characterized by a "push-pull" electronic effect [23,30]. The molecular structure or spatial arrangement of the donor and acceptor can be adjusted to modulate the electronic properties of the conjugated system, thereby influencing the fluorescent behavior [31].

Enhancing the electron-donating ability of donor or the electron-withdrawing ability of acceptor decreases the energy gap between the HOMO and LUMO, resulting in a redshift in absorption and emission wavelengths. Conversely, weakening these properties causes a blueshift. ICT-based fluorescent probes are highly sensitive to environmental changes, and their simplicity and well-defined mechanisms make them highly attractive for diverse applications, such as tuning emission colors and optimizing nonlinear optical properties.

2.2.4. *Aggregation-induced luminescence (AIE)*

Aggregation-induced luminescence (AIE), first described by Ben-Zhong Tang in 2001, contrasts with traditional aggregation-caused quenching (Fig. 1D) [32,33]. AIE materials exhibit negligible fluorescence in dilute solutions but significantly enhanced luminescence in aggregated states. Several theories have been proposed to explain AIE mechanisms, including excited-state intramolecular proton transfer (ESIPT), twisted intramolecular charge transfer (TICT), molecular charge transfer (MCT), and restriction of intramolecular motion (RIM). Among these, RIM is the most widely accepted, encompassing restricted intramolecular rotation (RIR) and restriction of intramolecular vibration (RIV) [34].

The degree of aggregation directly correlates with fluorescence intensity due to reduced non-radiative decay pathways. AIEgens are often applied in dense encapsulation forms, such as nanoparticles, amorphous polymers, or crystalline matrices. These forms minimize solvent effects

and optimize fluorescence performance, making AIE materials highly suitable for various applications including biomarker detection and imaging.

2.3. Fluorescent probe response modes

Fluorescent probes employ three primary sensing strategies for detection and analysis based on changes in fluorescence states: "Enhanced" (Turn-on) [35], "Quenched" (Turn-off) [36], and "Ratiometric" [37]. “Turn-on” fluorescent probes are initially non-fluorescent or exhibit very weak fluorescence, which becomes significantly enhanced in response to the target analyte. “Turn-off” fluorescent probes possess strong initial fluorescence that diminishes or disappears upon interaction with the target analyte. Ratiometric fluorescent probes usually utilize two fluorescent materials with distinct emission wavelengths, enabling dual-emission detection and ratio-based fluorescence analysis.

Among these strategies, “Turn-on” fluorescent probes offer several advantages, most notably their ability to establish a direct, linear relationship between fluorescence intensity changes and analyte concentration [38]. This characteristic enables highly sensitive and quantitative detection, where higher concentrations of the target analyte result in more significant fluorescence recovery within a specific range. However, “Turn-on” probes are often more susceptible to interference from environmental factors, such as temperature and pH fluctuations, as well as structurally similar substances in complex biological samples. These factors can lead to false-positive signals and compromise the reliability of the probes in detecting target analytes in complex or low-concentration environments. In contrast, “Turn-off” fluorescent probes are characterized by their simplicity in design, rapid detection capabilities, and cost efficiency. They typically exhibit lower susceptibility to environmental interference because they emit fluorescence in the absence of the target, which helps minimize background noise in certain contexts [39]. However, these probes may suffer from limitations in signal sensitivity, as their fluorescence intensity diminishes upon binding with the analyte, leading to less pronounced signal changes. This can hinder their performance, particularly in trace analysis, where the reduction in fluorescence may be difficult to detect accurately. Ratiometric fluorescent probes provide further enhancements by enabling self-calibration through the simultaneous measurement of fluorescence intensities at multiple wavelengths [40]. This dual-emission strategy significantly reduces the impact of environmental interferences, thereby improving both detection sensitivity and accuracy. Additionally, changes in fluorescence at different wavelengths often manifest as shifts in fluorescence color. Compared to variations in fluorescence intensity alone, these color changes are more visually discernible, simplifying the process of information reading and enhancing user-friendliness.

3. Different types of fluorescent nanomaterials

The fluorescence unit is pivotal in determining the sensitivity of a fluorescent probe, as its structural design and material composition directly influence the probe’s detection performance. An ideal fluorescent probe should exhibit strong affinity toward the target biomarker while minimizing interference from external environmental factors. Traditional fluorescent probes for biomarker detection and imaging predominantly used OFMs, such as coumarin, rhodamine, and cyanine [41–43]. These fluorophores are abundant and have fluorescence emission wavelengths spanning the visible spectrum (400–800 nm). However, the signals exhibited by these fluorophores are frequently vulnerable to interference from extraneous factors within the environment (such as pH and temperature) and instrumental errors (such as minor variations in excitation or emission intensities). The utilization of OFMs is also encumbered by several disadvantages, including their high photobleaching, low water solubility, narrow excitation spectra and broad emission spectra. These limitations hinder their application in high-sensitivity and high-accuracy rapid detection of biomarkers. Nanomaterials possess unique properties owing to their nanoscale size and structure, including quantum confinement effects, high specific surface area, and ease of interaction with other substances, providing new directions for fluorescent probe design for biomarkers detection and imaging. Therefore, fluorescent probes based on nanomaterials such as QDs, MNCs, CDs, and MOFs have attracted considerable significant attention in biomarker detection and imaging due to their high fluorescence quantum yield, superior photostability, and excellent biocompatibility (Table 1) [13,16,44].

3.1. Quantum dots (QDs)

QDs are small semiconductor nanoparticles ranging from 1 to 10 nm in size, typically composed of group II-VI, II-V, or IV-VI elements, such as ZnS QDs, CdS QDs, and InAs QDs [45,46]. Compared to OFMs, QDs exhibit several advantageous properties, including broad excitation spectra, narrow and symmetric emission peaks, excellent photostability, and long fluorescence lifetimes [47–49]. The reduced overlap of emission peaks in QDs with distinct fluorescence characteristics allows for interference-free coexistence in multi-fluorescence signal detection systems. These properties enable fluorescence detection even in low-signal-intensity environments by reducing the overlap between excitation and emission spectra, facilitating easier differentiation and identification of fluorescence signals. At the same time, the surface modification of QDs (Fig. 2A) and green synthesis can improve their photobleaching resistance and reduce toxicity to improve biomarker detection and imaging [50,51]. For instance, biomimetically synthesized RPL14B-based CdSe QDs demonstrated remarkable resistance to photobleaching, maintaining stable fluorescence intensity and consistent emission peaks even after repeated excitation cycles [52]. Meanwhile, a metal-enhanced fluorescence of CdSe@ZnS modification with SiO_2 biosensing platform has been developed for the detection of C-reaction protein (CRP) with good photobleaching resistance, low toxicity, and good biocompatibility [53]. The quantum yield of the CdSe@ZnS@SiO_2 core/shell QDs was found to be up to ~ 80 %, with type-I band alignment being employed to confine the carrier wave functions. The fluorescence intensity of the core-shell mechanism QDs was found to be further amplified by the localized surface plasmon resonance (LSPR) effect of the gold nanoparticles, which were able to detect CRP in the range of 0.5–100 ng/mL with a detection limit of 0.076 ng/mL. The development of QDs with core/shell structures through surface coating or modification has also proved effective in minimizing surface defects and increasing fluorescence quantum yield.

Although QDs with the core-shell structure have a higher quantum yield, the ligand molecules on the outer shell, which play a protective role, are usually susceptible to detachment or degradation under the influence of external factors or chemical reactions. As a result, their tolerance to environmental factors such as water, oxygen and heat is relatively low. Additionally, QDs are prone to agglomeration during use, which increases their size and adversely affects luminescence stability, potentially leading to structural degradation. Moreover, intrinsic toxicity and the complexity of surface functionalization remain significant obstacles to the broader application of QDs in biological and clinical applications.

3.2. Metal nanoclusters (MNCs)

MNCs are ultra-small nanoparticles with sizes typically less than 3 nm and well-defined molecular structures, positioning them between individual metal atoms and plasmonic metal nanoparticles [54,55]. Their size, which is close to the Fermi wavelength of electrons, results in discrete energy levels, a high specific surface area, and strong fluorescence [56,57]. The physicochemical properties of MNCs are determined by their metal cores and shell protection ligands (Fig. 2B) [58].

Table 1
Advantages and limitations of various fluorescence nanomaterials used in biomarkers detection and bioimaging applications. Adapted from Refs. [13,16].

Name	Quantum dots (QDs)	Carbon dots (CDs)	Metal nanoclusters (MNCs)	Metal-organic frameworks (MOFs)
Size	<10 nm	<10 nm	typically 1–3 nm	>50 nm
Advantages	• Tunable emission • Narrow and symmetric emission peak • Photostable • High quantum yield, long lifetime	• Biocompatible • Tunable emission • Small particle size • Low photobleaching • Photostable	• Large specific surface area • High conductivity • Good biological affinity • Photostable • Low toxicity	• High surface area • High porosity • Structural adjustability • Tunable compositions • Multifunctional
Disadvantages	• High toxicity • Large hydrodynamic size	• Low yield • Poor size control	• Difficult large-scale synthesis • Poor stability	• Poor reproducibility • Complex synthesis process

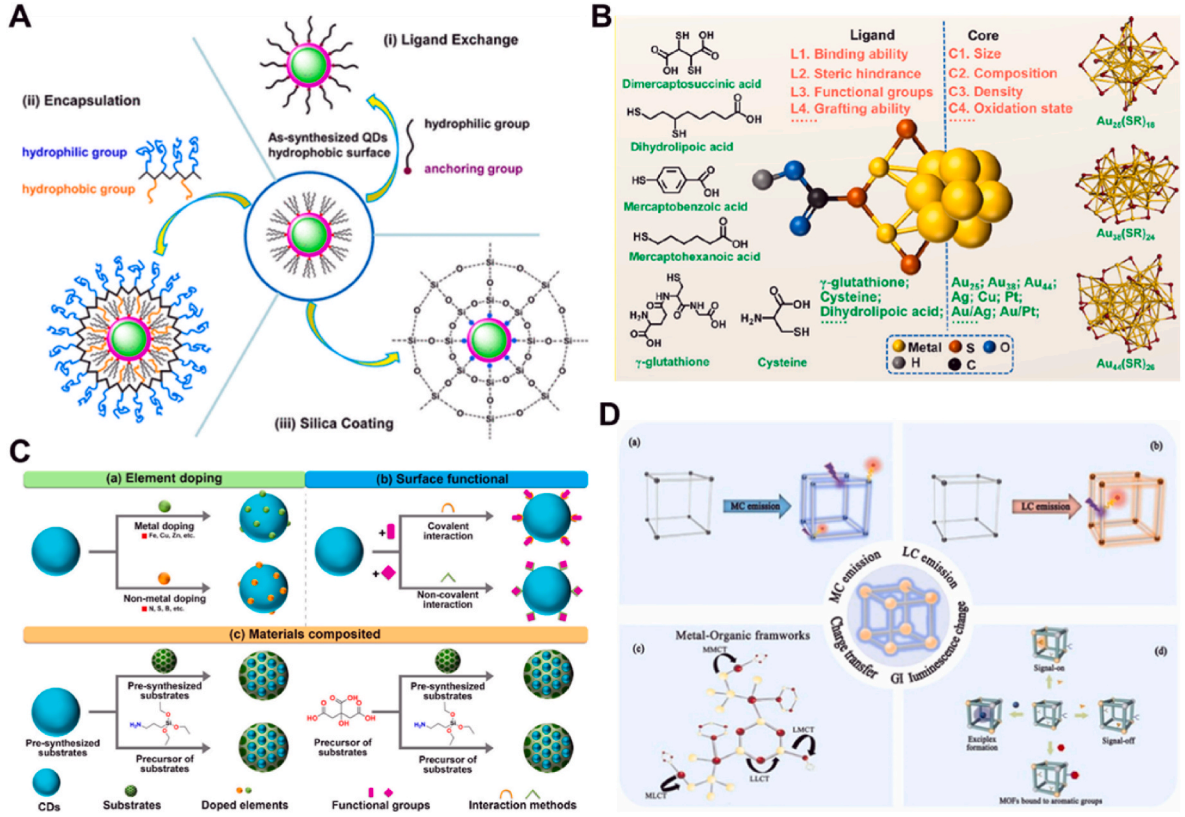

Fig. 2. Schematic diagram of functionalization or physicochemical properties of the nanomaterials for enhanced biomarkers detection and imaging. (A) Surface functionalization modification methods to make QDs colloidally stable in aqueous solution. (Reprinted with permission from Ref. [50]. Copyright 2016 American Chemical Society). (B) Schematic illustration of physicochemical properties of the "metal core–ligand shell" structure of MNCs. (Reprinted with permission from Ref. [58]. Copyright 2023 American Chemical Society). (C) Modification methods of CDs including element doping, surface modification and materials composited. (Reprinted with permission from Ref. [23]. Copyright 2023 American Chemical Society). (D) Four classifications of MOFs fluorescence mechanisms. (Reprinted with permission from Ref. [22]. Copyright 2023 Elsevier).

Specifically, the atomic structure of the metal core plays a critical role in their stability, with high-symmetry structures exhibiting greater binding energies and enhanced stability. MNCs are predominantly synthesized through template methods, where specific template molecules or stabilizers-such as thiols, DNA oligonucleotides, peptides, or proteins-are employed to improve their optical properties and stability [59]. The ligand shell structure on the surface of MNCs is vital for protecting the metal core, and fluorescence emission properties can vary significantly based on the protective ligands used, even when the same metal core is selected [60,61]. Common protective ligands for MNCs include sulfhydryl compounds, polymers, proteins, and DNA. Despite significant advancements, aqueous-phase MNCs often suffer from insufficient anti-aggregation stability and low resistance to ambient oxygen, while the application of organic-phase MNCs in biomedical fields remains limited. To enhance their performance, MNCs can be hybridized with other materials, such as graphene, biomolecules, or inorganic materials. Liu et al. developed the ratiometric fluorescent probes by integrating gold nanoclusters with photonic crystals to detect acetylcholinesterase and its inhibitor paraoxon [62]. The fluorescence intensity was further enhanced by leveraging the selectivity of photonic crystals.

Despite the potential of MNCs for clinical biomarkers detection and imaging, challenges persist in the broader application of these technologies. These challenges encompass biocompatibility, environmental sensitivity, and surface chemical stability, which collectively impede progress and widespread adoption in practical biomedical applications.

3.3. Carbon dots (CDs)

CDs are typically quasi-spherical nanoparticles with dimensions smaller than 10 nm. They generally consist of a carbon core (sp^2 carbon) surrounded by surface groups and post-modified functional groups [63]. One of the most remarkable properties of CDs is their fluorescence, characterized by broad emission peaks, large Stokes shifts, and an

abundance of functional groups, such as -OH, -CHO, -NH_2 and -SH on their surfaces and edges [64]. CDs offer significant advantages over conventional fluorescent materials, including excellent photostability and low toxicity [65–67]. The fluorescence characteristics of CDs are influenced by their internal microstructures and the chemical states of their surfaces, making modification a critical strategy for optimizing their optical properties. These modification strategies can be broadly categorized into heteroatom doping, surface functionalization, surface passivation, and materials composited (Fig. 2C) [23]. Heteroatom doping, the most widely used approach, involves replacing carbon atoms in the sp^2/sp^3 lattice with dopant elements such as nitrogen (N), boron (B), phosphorus (P), sulfur (S), or halogens [68,69]. This method not only introduces additional active sites on the CDs' surfaces but also alters their fluorescence emission wavelengths and quantum yields. For instance, doping with high-electronegativity elements (e.g., N, S) typically induces a blue shift in emission, whereas low-electronegativity elements (e.g., P, B) result in a red shift. Shao et al. synthesized nitrogen-sulfur co-doped CDs (NS-CDs) via a hydrothermal method, successfully employing them for fluorescence imaging of glutathione in living cells and zebrafish [70]. Surface functionalization further modulates the physical and optical properties of CDs by introducing new chemical groups, which enhance the electron cloud density, while potentially reducing original functional groups. Surface passivation, on the other hand, involves encapsulating CDs with passivators to stabilize the surface states and reduce the energy dissipation of photosensitive carriers, thereby improving fluorescence efficiency. Passivated CDs exhibit higher optical activity and improved enhanced fluorescence properties compared to their unmodified counterparts.

Due to their low toxicity, excellent biocompatibility, tunable emission properties, simple synthesis processes, and good water solubility, CDs have emerged as a promising class of fluorescent nanomaterials for biosensing applications. However, their clinical translation is still hindered by challenges such as limited reproducibility, consistency, and selectivity.

3.4. Metal-organic framework materials (MOFs)

MOFs are novel porous materials characterized by periodic network structures formed through the self-assembly of metal ions and organic ligands [71,72]. Compared to traditional porous materials, MOFs exhibit a large specific surface area, high porosity, structural tunability, and unique photofunctionality [73–75]. The luminescence mechanisms of MOFs are primarily attributed to metal ion luminescence, organic ligand luminescence, and electron-transfer luminescence processes, such as (a) metal-centered emission (MC); (b) ligand-centered emission (LC); (c) charge transfer (CT); (d) guest-induced luminescence change (GI) (Fig. 2D) [22]. Leveraging the ligand-to-metal CT (LMCT) fluorescence mechanism, Wang et al. synthesized "lab-on-MOFs" by adjusting the ratios of Eu^{3+}, Tb^{3+}, and Dy^{3+} metal ions and employing 5-boronoisophthalic acid (5-bop) as an organic ligand [76]. The MOFs exhibited distinct color changes upon interaction with various targets, including metal ions, anions, small molecules, and biomolecules, enabling multi-target substance detection. For non-fluorescent MOFs, fluorescent MOF materials can be prepared by encapsulating luminescent guests, such as quantum dots, metal complexes, or organic fluorophores. This method is straightforward and offers diverse tunable properties. The combination of MOFs with other fluorescent materials has been demonstrated to enhance electron-transfer processes, thereby increasing fluorescence intensity. For example, BZA-BOD@ZIF-90 has been developed for the detection of protamine and heparin by integrating MOF materials with AIE fluorescent molecules [77]. MOFs with intrinsic fluorescent sensing capabilities can also serve as ratiometric fluorescent probes when encapsulated with molecular fluorophores. Notably, when two fluorescent substances are encapsulated simultaneously within MOFs, the resulting dual-emission ratiometric fluorescent probes enhance detection accuracy. Wang et al. synthesized lanthanide-based Lu- and Y-MOFs and introduced Eu^{3+} and Tb^{3+} into Lu-MOFs to create dual-emission ratiometric fluorescent probes for the detection of antibiotics such as ornidazole and rotenazole [78]. The Y-MOF fluorescent probes were then successfully utilized to detect the antibiotic olanzapine and rotenazole, as well as autoantibodies against CRP.

MOFs offer significant advantages in the design of fluorescent probes due to their structural versatility and tunable pore sizes. However, their application in clinical detection remains constrained by challenges such as poor dispersion in aqueous solutions and difficulties in achieving precise structural control.

The biocompatibility of fluorescent nanomaterials is critical for their in vivo application in biomarker detection. Prior to clinical translation, it is essential to evaluate their metabolic pathways, immune responses, and potential for organ accumulation. Most inorganic fluorescent nanomaterials, such as gold nanoparticles (AuNPs), QDs and silica, are resistant to degradation and metabolism in vivo and can be stabilized in vivo for long periods of time [79,80]. But at the same time some inorganic nanoparticles degrade and release metal ions in the acidic environment of lysosomes, which then react with different biomolecules by oxidation, reduction and binding. For instance, silver nanoparticles (AgNPs) may undergo metabolism via two primary routes: dissolution to release Ag^+ ions or transformation into silver sulfide (Ag_2S) [81]. Meanwhile, larger nanoparticles (>200 nm) tend to accumulate in the liver and spleen via the mononuclear phagocyte system, and medium-sized nanoparticles (10–200 nm) are able to be distributed more readily in various tissues, whereas smaller particles (<10 nm) are more readily eliminated via renal excretion [82]. For example, a multicolored fluorescent silicon-containing nanodots (SiNDs) with a size below 5 nm exhibited a renal clearance efficiency of up to 86 % within 12 h [83]. The immunogenicity of nanomaterials can be influenced by factors such as surface charge, morphology, and surface modifications. Notably, PEGylation of the nanoparticle surface has been shown to significantly reduce immune activation and improve biocompatibility [84]. In summary, the metabolic fate, immune response, and organ accumulation of nanomaterials are closely related to their physicochemical properties, including surface chemistry, size, and composition. Several comprehensive reviews have addressed these aspects in detail and may be referred to for further reading [80,82,85–87]. Nonetheless, a thorough assessment of biocompatibility remains imperative before these fluorescent nanomaterials can be applied in clinical biomarker detection.

4. Application of fluorescent nanomaterials probes

Biomarkers are a diverse group of entities, including small molecules such as amino acids and metabolites, biomacromolecules such as proteins, DNA, and RNA, as well as other categories such as metal ions, bacteria, and circulating tumors cells (CTCs). The following concise overview provides the application of fluorescent nanomaterials probes in the detection and imaging of disease-associated biomarkers (Table 2).

4.1. Small molecules detection and imaging

Hydrogen sulfide (H_2S) is a toxic gas with a characteristic rotten-egg odor that plays a crucial role in numerous physiological and pathological processes of organisms, including vasodilation, angiogenesis, inflammation and apoptosis. Dysregulated levels of H_2S have been implicated in various diseases such as diabetes, Down's syndrome, and cirrhosis. Xiang et al. developed a ratiometric fluorescent probe, RBDA, based on gold nanoclusters (AuNCs) for detecting H_2S in living organisms [88]. The probe leveraged the modulation of the surface structure of AuNCs by H_2S, inducing fluorescence emission via a two-stage kinetic reaction process to achieve highly sensitive detection. In Stage I, H_2S facilitated surface Au(I)-ligand reduction and Au(0) core growth, resulting in rapid fluorescence quenching; stage II involved the optimization and reconstruction of the surface structure, accompanied by

Table 2
Selected examples of fluorescent nanomaterials for biomarker detection and imaging.

Biomarker	Nanomaterial	Size	Quantum yield	Bioimaging application	Ref.
Superoxide anion ($O_2^{\bullet-}$)	Activatable polymeric nanoprobe (APN_{SO})	≈160 nm	1.8 %	Real-time imaging of living mice with hepatic ischaemia-reperfusion injury.	[12]
Peroxynitrite ($ONOO^-$)	CD–N-I	–	26 %	Imaging of exogenous and endogenous $ONOO^-$ in live cells.	[107]
Hydrogen sulfide (H_2S)	DCNP-Cu_2O@PDA	≈40 nm	–	In vivo NIR-II imaging of H2S in colon cancer of mice.	[108]
Dopamine	CDs	1–5 nm	21 %	NCFM image of dopamine in MDA-MB 468 cells.	[91]
Ascorbic acid (AA)	g-C3N4/BSA@MnO2	~86.27 nm	–	Imaging of exogenous AA in raw macrophage cells.	[93]
Carcinoembryonic antigen (CEA)	CEA(Ab)-MSNs-ICG-Pt	~300 nm	–	In vivo NIR imaging of RKO xenografts.	[109]
Flap endonuclease 1	Biomineralized ZIF-8 NPs	~92 nm	–	Direct imaging of FEN1 in living cells	[110]
Carboxylesterase 1 (CES1)	LysFP@ZIF-8	–	0.76	Visual monitoring of CES1 activity in living cells.	[111]
HER2	GQNP-Herceptin	43–51 nm	–	Imaging of SK-BR3 cell	[97]
RNA	Red-emissive carbon dots	1.6 nm	22.83 %	RNA labeling and SG dynamics imaging in live cells.	[112]
miRNA-221 and caspase-3	COF–H1/H2-Peptide	~160 nm	–	Confocal laser scanning microscopy images of HeLa cells.	[113]
Fe^{3+}	ZIF-90	122 ± 35.47 nm	–	Imaging of Fe^{3+} in HepG2 cells.	[102]
Bacteria	$NaYF_4$:Nd,Yb@$NaYF_4$ (csNd,Yb) and $NaYF_4$:Yb,Er,Ce@$NaYF_4$ (csYb,Er,Ce)	21.45 ± 0.95 nm (csNd,Yb), 33.99 ± 1.03 nm (csYb,Er,Ce)	–	Imaging and identification of bacterial infection.	[114]
Candida albicans	Sulfur-doped CDs (S-CDs)	~1.6 nm	~78 %	Confocal fluorescence images of live and dead *C. albicans* cells.	[103]
Exosomes	Semiconductor polymer dots	12 nm	–	In vivo imaging of exosomes in liver-injured mice.	[115]
Circulating tumor cells (CTCs)	CD@NM	3–5 nm	–	In vivo fluorescence images of mice and ex vivo fluorescence images of tissues.	[106]

slower fluorescence quenching. The RBDA probe utilized FRET between AuNCs and rhodamine B, achieving a proportional fluorescence response with high sensitivity, selectivity, and biocompatibility. The probe was successfully applied to monitor H_2S levels in living cells and zebrafish, demonstrating excellent biostability and low cytotoxicity (Fig. 3A). Additionally, a green-orange dual-color emission sulfur co-doped fluorescent carbon dots (DE-CDs) system was synthesized using a simple hydrothermal method for pH and H_2S sensing, as well as bioimaging [89]. The fluorescence intensity of DE-CDs increased with rising pH values due to deprotonation. Furthermore, H_2S acted as an enhancer for fluorescence emission, achieving a linear detection range of 25–500 μM and a limit of detection (LOD) of 9.7 μM. The DE-CDs demonstrated excellent photostability, low toxicity, and biocompatibility, making them effective for H_2S imaging in HeLa cells and zebrafish.

Reactive oxygen species (ROS) are a class of oxidative molecules (e.g., ClO^-, H_2O_2, $ONOO^-$) produced during cellular metabolism. At low concentrations, these molecules function as signaling mediators; however, excessive accumulation of ROS can lead to cellular damage and even cell death. Abnormal ROS levels are intricately linked to various pathophysiological processes, including oxidative stress, inflammatory responses, and apoptosis. Jiang et al. developed innovative multicolored fluorescent silicon-containing nanodots (SiNDs) using a one-step hydrothermal method [83]. These SiNDs exhibited tunable fluorescence (blue (bSiNDs), green (gSiNDs), and red (rSiNDs)) achieved by varying the type of silane reagent or dye molecule. The gSiNDs demonstrated a high quantum yield of up to 72 %. To monitor H_2O_2 levels in vivo, gSiNDs@MnO_2 core-shell nanoprobes were fabricated. These nanoprobes exhibited fluorescence enhancement in the presence of H_2O_2 and were successfully employed for real-time imaging of H_2O_2 levels in HepG2-xenograft tumor models. Compared to near-infrared region I (NIR-I, tissue penetration depth typically <1 cm), near-infrared region II (NIR-II) offers significantly greater tissue imaging depth, making NIR-II nanomaterial-based fluorescent probes highly attractive for biomarker detection and imaging. Recently, NIR-II nanoparticles (PSMA@IR1048 NPs) were synthesized by encapsulating the NIR-II fluorescent molecule IR1048 in poly(styrene-co-maleic anhydride) (PSMA) [90]. Using a charge modulation strategy, NIR-II ratiometric fluorescent nanomaterial probes (RNPs, including RNP1, RNP2, and RNP3) were constructed by loading cyanine fluorophores onto the surface of PSMA@IR1048 NPs. Among these, RNP2 demonstrated a strong NIR-II fluorescence ratiometric signal (FL2/FL1) in the presence of HClO, enabling its sensitive detection. The nanoprobes were effectively applied to NIR-II fluorescence imaging of diabetes-induced liver injury and lower limb ischaemia-reperfusion (I/R) injury in live mouse models (Fig. 3B), showcasing significant potential for disease diagnosis and monitoring.

Dopamine (DA) is a vital neurotransmitter in mammals, playing an essential role in the nervous and cardiovascular systems. Abnormal DA secretion is strongly associated with numerous diseases, including Parkinson's disease, Huntington's chorea, Alzheimer's disease, and pheochromocytoma. Kumar et al. synthesized fluorescent CDs from porcine pancreatic lipase for DA detection via FRET and live cell imaging [91]. These CDs exhibited a quantum yield of 21 % in aqueous solution and an LOD for DA of 20 nM. The CDs also enabled successful imaging of DA in MDA-MB 468 cells with low cytotoxicity (Fig. 3C). Recently, a novel fluorescent nanomaterial based on Cr^{3+}-doped zinc gallate ($ZnGa_2O_4$:Cr^{3+}, ZGC) luminescent nanoparticles, modified with mesoporous zeolite imidazole frameworks (ZIF-8-NH_2), was proposed for non-invasive fluorescence detection of DA [92]. This ZGC/ZIF-8-NH_2 probe achieved an LOD of 0.075 μM for DA in urine, with a detection range of 0–4 μM. Furthermore, the probe was incorporated into a chitosan-based hydrogel patch for sensitive and accurate detection of DA in sweat through a smart sensing platform. This approach eliminated the need for complex sample pre-treatment and achieved recovery rates ranging from 95.3 % to 108.7 %.

Metabolites are the ultimate products of pathological and physiological changes, regulating numerous cellular activities such as signaling and energy transfer. Fluctuations in metabolite levels can accurately reflect the state of biological systems. For instance, a deficiency in ascorbic acid (AA) can lead to colds, scurvy, and even cancer, while excessive levels of AA may result in urinary stones, diarrhea, and hyperacidity. Thus, the accurate detection of AA is of significant clinical

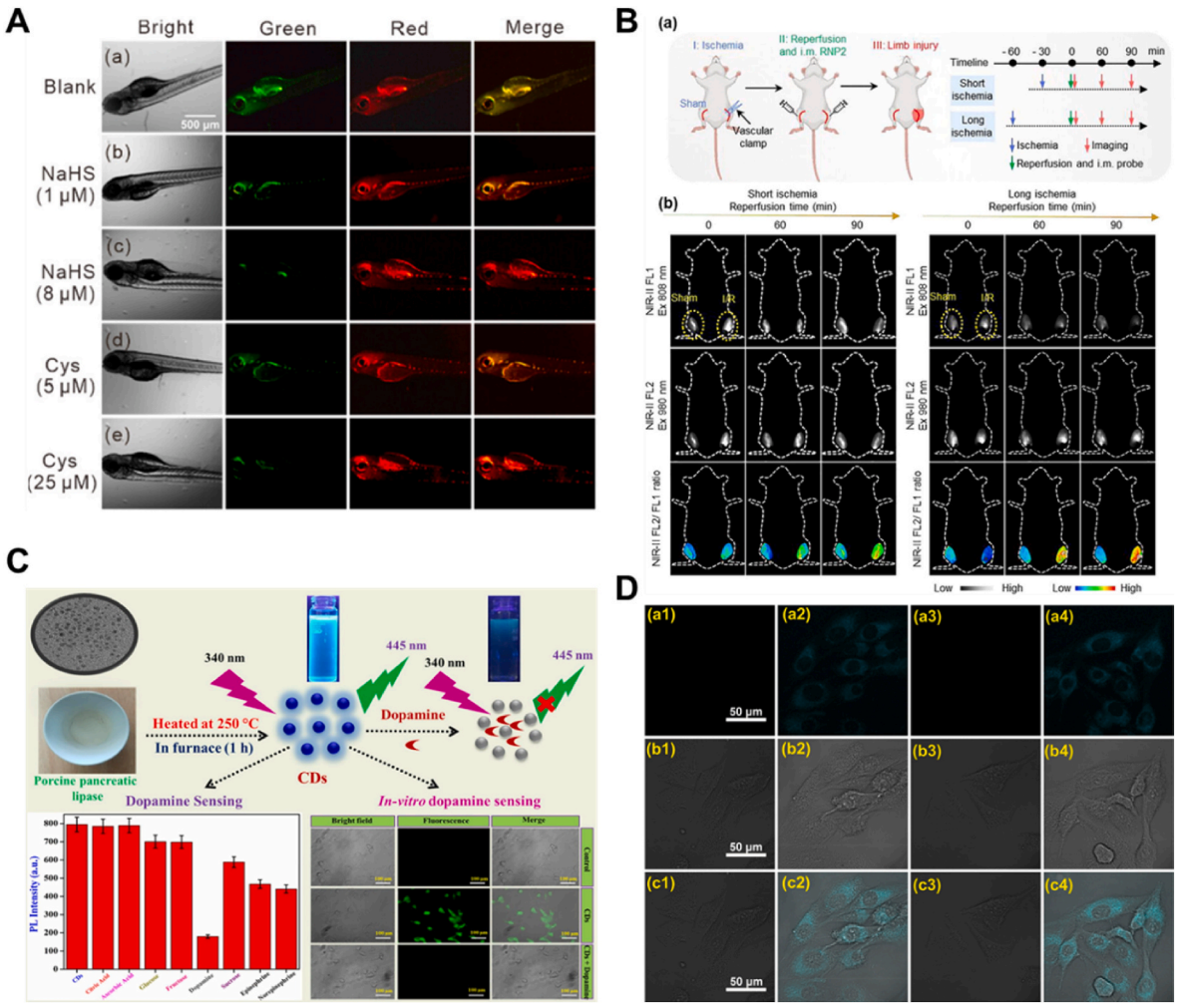

Fig. 3. Small biomolecules detection and imaging based on the fluorescent nanomaterials. (A) Fluorescence imaging of exogenous and endogenous H_2S in zebrafish based on AuNCs. (Reprinted with permission from Ref. [88]. Copyright 2023 American Chemical Society). (B) Representative steps of the I/R process in the lower limb. Long-term ischaemia: 60 min ischaemia; transient ischaemia: 30 min ischaemia. (b) FL1, FL2 and FL2/FL1 ratio images of short and long-term ischaemic mice after intramuscular injection of RNP2 for 0, 60 and 90 min. Emission wavelength: 1100–1700 nm. Yellow curves indicated sham-operated and I/R regions. (Reprinted with permission from Ref. [90]. Copyright 2023 Elsevier). (C) Fabrication of CDs from PPL and applied for the detection and in vitro cellular imaging of dopamine. (Reprinted with permission from Ref. [91]. Copyright 2020 Elsevier). (D) Fluorescent imaging of Fe^{3+} and AA in living MG-63 cells by the CDs. (Reprinted with permission from Ref. [94]. Copyright 2022 Tsinghua University Press). (For interpretation of the references to color in this figure legend, the reader is referred to the Web version of this article.)

importance. Sun et al. developed a nanomaterials-based probe (g-C_3N_4/BSA@MnO_2) composed of graphite-phase carbon nitride (g-C_3N_4) nanosheets and manganese dioxide (MnO_2) nanocomposites coated with bovine serum albumin (BSA) for the detection and imaging of AA in living cells [93]. In this composite material, the fluorescence of g-C_3N_4 nanosheets was quenched by BSA@MnO_2 nanoparticles via FRET. Upon the presence of AA, an oxidation-reduction reaction occured with MnO_2, leading to its degradation, which eliminated the FRET effect and restores fluorescence. This "on-off" mechanism enabled sensitive fluorescence-based detection of AA. The probe demonstrated a linear response to AA within the range of 0–120 μM, with a detection limit of 133 nM. Furthermore, it was successfully applied for fluorescence imaging of exogenous AA in RAW cells, showcasing excellent selectivity and stability. Additionally, a green synthesis approach was proposed to fabricate carbon dots (CDs) for the selective and quantitative detection of Fe^{3+} and AA via a fluorescence "on-off-on" mechanism [94]. These CDs were prepared using precursors such as polyvinylpyrrolidone, citric acid, and methionine. The CDs exhibited high sensitivity for Fe^{3+} detection within the range of 0.001–0.8 mM and for AA detection within the range of 0.01–50 mM, with detection limits of 0.26 nM and 17.6 μM, respectively. Leveraging their remarkable water solubility and biocompatibility, the CDs were effectively used for imaging and tracking Fe^{3+} and AA in live cells (Fig. 3D).

4.2. Biomacromolecules detection and imaging

Proteins are essential executors of human life activities, and their proper functioning is vital for all biological processes. Abnormal protein expression during various biological events can serve as an indicator of disease onset, and its detection is critical for disease prevention, early diagnosis, therapeutic evaluation, and ultimately, reduction of mortality. Carcinoembryonic antigen (CEA) is a glycoprotein-polysaccharide complex associated with cell adhesion, commonly found in ovarian, colon, gastric, breast, and lung cancers. A targeted biodegradable near-infrared fluorescent silicon nanoparticle (FSN) system was developed for the detection and imaging of colorectal cancer (CRC) [95]. Utilizing an EDC-NHS coupling reaction, CEA antibodies were conjugated to PEGylated FSNs, thereby forming CEA-functionalized FSNs (CEA-FSNs). The valuation employing the F344-PICC rat model demonstrated that following the identification of intestinal polyps via white light

endoscopy, local application of CEA-FSNs enabled the detection of near-infrared fluorescence signals in excised intestinal tissues. Immunofluorescence imaging confirmed co-localization of CEA-FSNs with CRC and CEA signals, emphasizing their potential as molecular imaging markers for CRC detection and diagnosis. Similarly, alpha-fetoprotein (AFP) is a glycoprotein synthesized by fetal liver cells and the yolk sac and is widely used as a biomarker for diagnosing liver cancer. To enhance the detection and imaging of CEA and AFP, a biotin-streptavidin (Bio-SA) amplified QDs fluorescent immunosensor was developed [96]. This platform leveraged the high affinity and minimal steric hindrance of the Bio-SA system, enabling highly sensitive detection of AFP and CEA with detection limits of 0.18 ng/mL and 0.08 ng/mL, respectively. Additionally, the biosensor demonstrated excellent performance in cellular imaging, yielding brighter fluorescence signals while the modified QDs exhibited low toxicity, offering a robust tool for imaging and tracking cancer cells such as RAW264.7, HCT116, or SW480 cells (Fig. 4A). Moreover, the cost of the primary antibody used in this platform has been reduced by 80–90 %, significantly lowering the overall cost of biomarker detection. This innovation represents a promising advancement in cancer diagnostics and imaging based on fluorescent nanomaterials probes.

Membrane proteins are key mediators of the biological functions of cell membranes, playing critical roles in signal transduction, molecular transport across membranes, and cell recognition and interaction. During cancer progression, the overexpression or dysregulated secretion of certain membrane proteins by cancer cells or the tumor microenvironment significantly influences tumor cell growth, survival, and migration. Detection of membrane protein biomarkers is therefore crucial for early disease diagnosis. For instance, HER2 (human epidermal growth factor receptor 2) is overexpressed in approximately 25 % of breast cancer cases, therefore monitoring HER2 expression is critical for the early diagnosis and therapeutic management of breast cancer. A fluorescence immunosensor based on graphene quantum dots (GQNPs) and magnetic nanoparticles (MNPs) was been developed for the detection of HER2-positive breast cancer cells [97]. This biosensor demonstrated high sensitivity and specificity toward SK-BR3 cells (HER2-positive), with a detection limit as low as 1 cell/mL and a rapid detection time of just 30 min. Vascular endothelial growth factor (VEGF) is a critical signaling molecule involved in intercellular communication and tumor metastasis, playing a pivotal role in tumor angiogenesis. Cong et al. developed a microfluidic droplet-based fluorescence imaging platform for analyzing VEGF secretion at the single-cell level [98]. The core of this

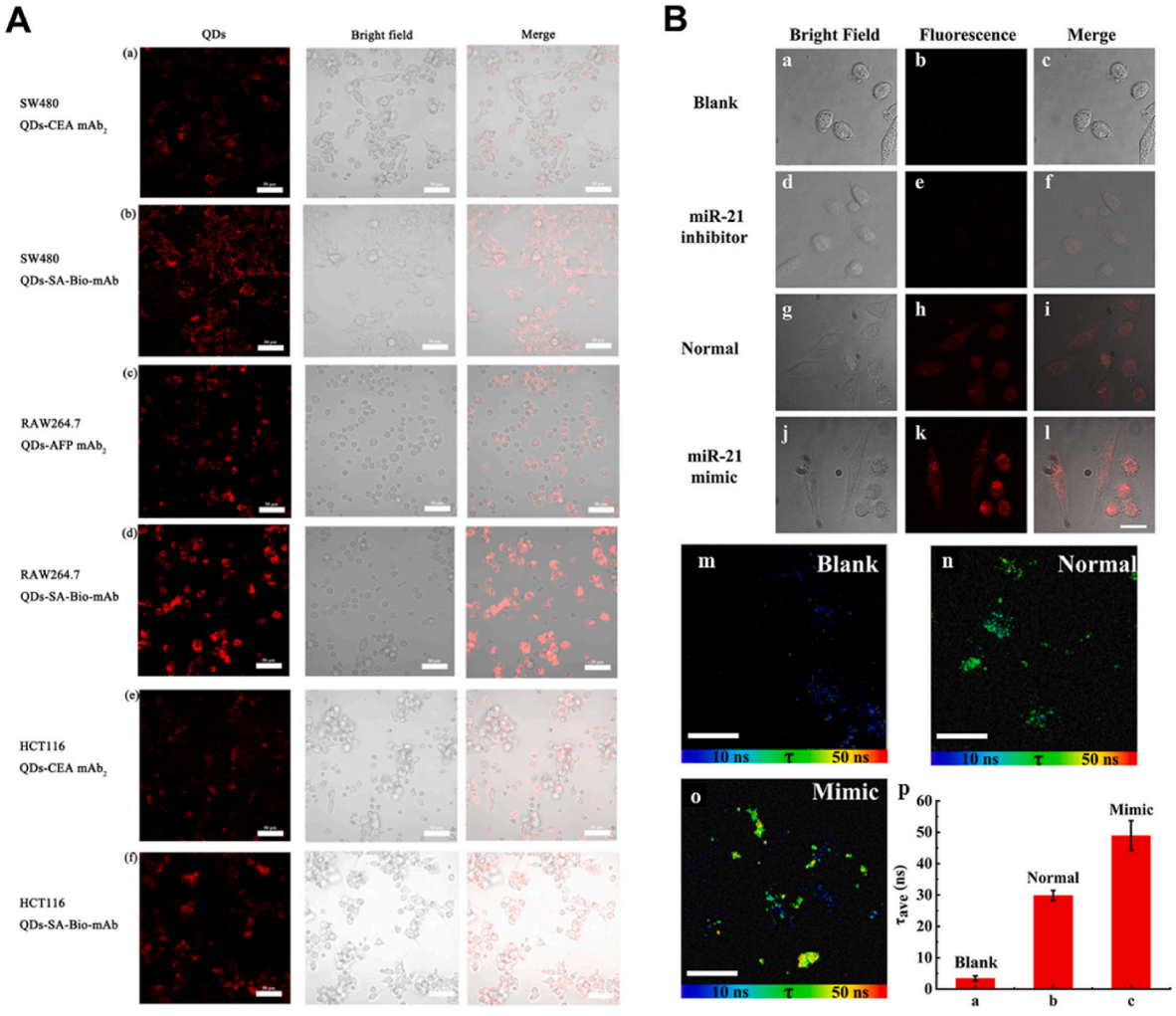

Fig. 4. Biomacromolecules detection and imaging based on the fluorescent nanomaterials. (A) CLSM imaging of SW480 cells with the QDs-mAb probe (a), RAW264.7 cells (c), and HCT116 cells (e), and QDs-SA-Bio-mAb probe in SW480 cells (b), RAW264.7 cells (d), and HCT116 cells (f). Scale bar = 50 μm. (Reprinted with permission from Ref. [96]. Copyright 2024 Elsevier). (B) TP of endogenous miRNA-21 in intact MCF-7 cells used AuNCs@SiO2-BHQ2-GO (140.0 μg/mL, 4.0 h). (a–c): blank MCF-7 cells. (d–f): inhibitor-treated MCF-7 cells. (g–i): untreated MCF-7 cells. (j–l): MCF-7 cells were treated with mimics of miRNA-21. FLIM of endogenous miRNA-21 in intact MCF-7 cells based on AuNCs@SiO2-BHQ2-GO (140.0 μg/mL, 4.0 h). (m) Blank MCF-7 cells. (n) Untreated MCF-7 cells. (o) miRNA-21 mimic treated cells. Scale bar = 25.0 μm. (p) Fitting values of fluorescence lifetimes of endogenous miRNA-21 in intact MCF-7 cells. (Reprinted with permission from Ref. [99]. Copyright 2023 American Chemical Society).

technology involved the use of two silica nanoparticle (SiO_2)-based immunoprobes: (1) dual-functional, non-fluorescent SiO_2 nanoparticles (SiO_2@Biotin-Ab/mAb_{VEGF}) designed to capture VEGF, and (2) dye-doped fluorescent SiO_2 nanoparticles with an anti-VEGF polyclonal antibody (F-SiO_2@pAb_{VEGF}) that emitted fluorescence signals. Through the construction of an immunosandwich structure on the cell surface, VEGF acted as a bridge connecting the capture and reporter probes, enabling sensitive and specific VEGF detection. The results demonstrated that cancer cells (MCF-7 and HeLa cells) secreted significantly higher levels of VEGF compared to normal cells (H8 cells). These findings highlighted the platform's capability for effective detection of VEGF secretion at the single-cell level, providing valuable insights into cellular heterogeneity and advancing cancer research.

Nucleic acids carry a wealth of biological information that can directly reflect biological regulation and disease progression. MicroRNAs (miRNAs) are endogenous, non-coding, highly conserved, single-stranded small RNAs whose dysregulated expression is closely associated with various human diseases, particularly cancer. For example, miRNA-21 is released into the bloodstream during breast cancer development, with its levels significantly upregulated in the early stages of the tumor. Li et al. developed a dual-mode detection platform for intracellular endogenous miRNA-21 based on silica-coated gold nanoclusters (AuNCs@SiO_2) coupled with nucleic acid probes [99]. This platform integrates two-photon (TP) fluorescence imaging and fluorescence lifetime imaging (FLIM) for enhanced detection (Fig. 4B). The use of BHQ2 and graphene oxide (GO) as dual fluorescent bursting agents significantly improved the signal-to-noise ratio and anti-interference capabilities, resulting in high sensitivity and selectivity for miRNA-21 detection in vitro, with a LOD of 0.91 nM. The dual-mode nanoprobes successfully enabled TP fluorescence imaging and FLIM of endogenous miRNA-21 in MCF-7 cells. TP fluorescence imaging outperformed single-photon fluorescence imaging in terms of sensitivity, with deeper tissue penetration (330.0 μm depth) and higher spatiotemporal resolution. Furthermore, FLIM effectively mitigated issues related to fluorescence intensity fluctuation and autofluorescence interference, providing an average fluorescence lifetime of 50.0 ns. The CRISPR-Cas12a system, known for its unique signal amplification properties, has been used for miRNA detection in vitro. However, its application in cellular imaging has been limited due to its complex composition and challenges associated with intracellular delivery. Recently, a CoOOH nanoflake-based CRISPR-Cas12a system was proposed for detecting and imaging miRNA-21 in cells [100]. In the presence of AA, CoOOH nanoflakes were reduced to Co^{2+}, which activates the CRISPR-Cas12a system for miRNA-21 detection. When the target miRNA-21 was recognized, the trans-cleavage activity of Cas12a was triggered, resulting in the cleavage of a reporter molecule and fluorescence emission. The CoOOH nanoflake-based CRISPR-Cas12a (CCS) probe exhibited excellent linearity for miRNA-21 detection in the concentration range of 0.5–50 pM and 100 pM-20 nM, with a detection limit of 0.32 pM. In HUVEC, MCF-7, and HeLa cells, the CCS probe displayed low cytotoxicity and remarkable cell imaging ability, effectively detecting intracellular miRNA-21 expression. These advances in miRNA detection highlight the potential of combining nanotechnology with CRISPR-based systems for high-sensitivity, non-invasive biomarker detection and imaging in cellular contexts.

4.3. Other biomarkers detection and imaging

Metal ions are omnipresent in the natural environment, and their detection plays a critical role in both environmental and biomedical applications. Alterations in the concentration of specific metal ions can reflect pathological states in the human body, offering potential tools for early diagnosis and disease monitoring. For instance, iron ions (Fe^{3+}) are essential for various physiological processes, including cellular respiration, tissue metabolism, and hemoglobin production. An imbalance in Fe^{3+} levels can disrupt the body's metabolic system, leading to conditions such as iron-deficiency anemia, cardiovascular diseases, and renal injury. Chang et al. developed bright blue fluorescent carbon-based CDs from the stem of Caulis polygoni multiflora using a one-step hydrothermal method for Fe^{3+} detection in vitro and in vivo [101]. The resulting carbon dots exhibited excitation-dependent fluorescence with a quantum yield of up to 42 %. The fluorescence of these CDs was significantly quenched by the static burst effect of Fe^{3+}, with a linear detection range from 0 to 400 μM and a LOD of 0.025 μM. These CDs were further applied to bioimaging of zebrafish larvae and nude mice, enabling real-time detection of Fe^{3+} concentration changes, while demonstrating good biocompatibility and low toxicity. More recently, a novel fluorescent nanoprobe, ZIF-90@FSS, and its paper-based nanofiber platform for Fe^{3+} detection and imaging were proposed [102]. The ZIF-90@FSS nanoprobe was synthesized by loading fluorescein sodium (FSS) into the pores of the ZIF-90 framework. ZIF-90 acted as a carrier, while FSS served as the fluorescent material, enabling fluorescence "off" detection in the presence of Fe^{3+}. The ZIF-90@FSS nanomaterials probes showed a good linear response in the concentration range of 0–150 ng/mL, with a detection limit as low as 0.26 ng/mL, making it highly sensitive for Fe^{3+} detection. Furthermore, the ZIF-90@FSS nanomaterial probe was successfully employed for fluorescence imaging of Fe^{3+} in HepG2 cells, enabling real-time monitoring of Fe^{3+} fluctuations within the cells (Fig. 5A). This platform provided a promising tool for studying the molecular transport mechanisms of intracellular Fe^{3+}-related proteins and held great potential for disease monitoring. These advancements in Fe^{3+} detection highlight the increasing utility of nanomaterial-based probes in both diagnostic and therapeutic applications, offering novel insights into metal ion regulation in biological systems.

Bacteria are intricately linked to human health, and the proliferation of pathogenic bacteria poses a significant threat, particularly in cases of sepsis, which can be caused by a variety of pathogens such as *Streptococcus pneumoniae*, *Hemophilus influenzae*, and *Neisseria meningitidis*. Yu et al. developed ultra-small (~1.6 nm), ultra-bright (~78 % quantum yield), and excitation wavelength-independent sulfur-doped CDs (S-CDs) for the rapid and accurate differentiation between living and dead cells (Fig. 5B) the rapid and accurate differentiation between living and dead cells) [103]. The S-CDs were synthesized using rose bengal as a precursor and 1,4-dimercaptophenyl as a stabilizing agent. These ultra-small S-CDs demonstrated excellent performance in distinguishing live from dead bacterial cells. The S-CDs efficiently penetrated the surface of dead cells, interacting with intracellular DNA/RNA and facilitating the staining of these cells. After a brief 5-min incubation, both Gram-positive *Staphylococcus aureus* (*S. aureus*) and Gram-negative *Escherichia coli* (*E. coli*) dead bacterial cells emitted strong fluorescent signals, while live bacterial cells remained unstained. This rapid, selective staining capability highlighted the potential of S-CDs for effective live/dead differentiation in bacterial populations. A multifunctional biomimetic therapeutic nanoparticle, RBC-O_2/TQ@PB, with aggregation-induced second near-infrared emission, sarcoidosis-targeting, and self-oxygenation properties, was proposed for combined phototherapy of tuberculosis [104]. Fluorescence imaging revealed that, under laser irradiation, RBC-O_2/TQ@PB significantly inhibited the growth of *Mycobacterium marinum* and bacillus Calmette-Guerin (BCG). Notably, the bacterial killing effect under light irradiation was markedly enhanced compared to treatment with laser irradiation or nanoparticles alone, suggesting a synergistic effect between the two modalities. In a tail granuloma mouse model, RBC-O_2/TQ@PB demonstrated optimal targeting ability at 24 h post-administration, remaining localized in the granuloma after 48 h, indicating its strong granuloma-targeting capability. Moreover, in the mouse model of BCG-induced pulmonary tuberculosis, RBC-O_2/TQ@PB was predominantly distributed in the liver, kidneys, and lungs, with a significant enhancement in its accumulation and targeting within lung granulomas compared to unmodified nanoparticles. These results suggested that RBC-O_2/TQ@PB nanoparticles possess promising

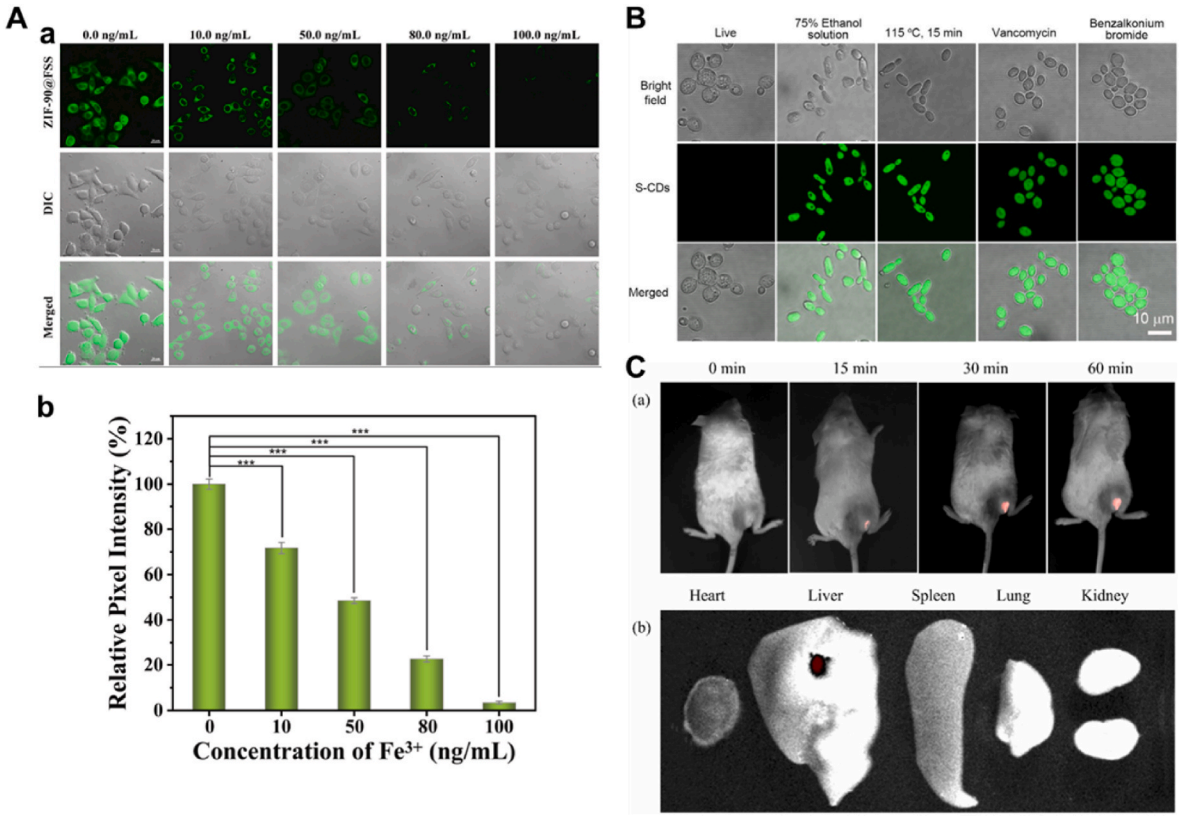

Fig. 5. Other biomarkers detection and imaging based on the fluorescent nanomaterials. (A) (a). Fluorescence imaging of Fe^{3+} in HepG2 cells based on the ZIF-90@FSS nanoprobe, scale bar: 20 μm. (b). Relative pixel intensity of live cells (n = 6). (Reprinted with permission from Ref. [102]. Copyright 2024 Elsevier). (B) Fluorescence images of live *C. albicans* cells and dead *C. albicans* cells stained with S-CD (20 μg/mL). (Reprinted with permission from Ref. [103]. Copyright 2022 American Chemical Society). (C) In vivo or ex vivo fluorescence images of mice based on CD@NMs at various time points or representative tissues at 12 h post-injection. (Reprinted with permission from Ref. [106]. Copyright 2023 Elsevier).

therapeutic and diagnostic potential for tuberculosis treatment and targeted bacterial therapies. This research illustrated the utility of nanomaterial-based platforms in distinguishing bacterial cell viability and in enhancing the targeting and therapeutic efficacy of drug delivery systems in infectious diseases.

CTCs are various types of tumor cells that are shed from primary tumor lesions and invade the circulatory system. These cells are closely associated with many types of cancers and serve as valuable biomarkers for disease progression and prognosis in tumor patients. Zhao et al. designed a combined strategy using octreotide-2,2′,2″,2‴-(1,4,7,10-tetraazacyclodecane-1,4,7,10-tetrayl) tetraacetic acid-modified magnetic Fe_3O_4 nanoparticles and signal-amplifying CDs@SiO_2 nanospheres for fluorescent cellular sensors aimed at capturing and detecting Pheochromocytoma CTCs (PCC-CTCs) in peripheral blood [105]. In this approach, target cells were isolated and enriched using a magnetic capture probe (Fe_3O_4-DOTA). Subsequently, the signaling probe (CDs@SiO_2-DOTA) was specifically bound to the target cells, forming a sandwich-like structure that allowed for fluorescent signal output. The fluorescent cell sensor demonstrated good linearity and a low detection limit of 2 cells/mL for PC12 cells, exhibiting high sensitivity and selectivity for PCC-CTCs. Moreover, when varying numbers of PC12 cells were added to healthy human peripheral blood samples, the fluorescence signal was progressively enhanced with the increasing number of PC12 cells. This results indicated that the fluorescent biosensor has good reliability and stability even in complex biological matrices. Given the low abundance of CTCs in blood, Ren et al. also proposed a nanomaterial-based platform, CD@NMs, to improve the separation efficiency of CTCs [106]. This material consisted of γ-Fe_2O_3 nanorods as the core, with folic acid (FA) and hyaluronic acid (HA)-modified CDs on the outer surface, acting as targeting ligands. The capture efficiency of CD@NMs for CTCs was 87.50 ± 3.88 % under the influence of a magnetic field. Moreover, the capture efficiency was significantly enhanced to 97.50 ± 2.38 % in the presence of 10 mM H_2O_2 and the magnetic field. In vivo tumor imaging experiments in mice further demonstrated the ability of CD@NMs to achieve specific imaging of tumor tissues, with no significant fluorescent signals detected in other major organs (Fig. 5C). This study underscored the potential of nanomaterial-based platforms in the sensitive and selective detection of CTCs, offering a promising tool for early cancer diagnosis and monitoring. The combination of magnetic capture and fluorescence signal amplification enhanced the efficiency and reliability of CTC separation and imaging, especially in complex biological environments.

5. Conclusion and future perspectives

In conclusion, fluorescent nanomaterials have become a powerful tool for high-sensitivity detection and imaging of biomarkers due to their unique physicochemical properties, such as high quantum yield, tunable optical properties, excellent stability and good biocompatibility. Recent advancements in nanomaterials have significantly improved the performance of fluorescent probes, particularly in the selective detection of small molecules, biomacromolecules, and various other biomarkers. In this review, we discussed the underlying fluoresce mechanisms, explored different types of fluorescent nanomaterials, and highlighted their applications in biomarker detection and imaging.

Although significant progress has been made in fluorescent nanomaterials for biomarker detection and imaging, the following challenges still need to be addressed: (1) Biocompatibility: Despite the promising applications of nanomaterials in biomarkers detection and imaging, their cytotoxicity and potential immune responses remain significant

barriers to clinical use. The development of biodegradable or naturally derived nanomaterials, along with comprehensive biocompatibility studies, should be prioritized to meet the safety standards required for in vivo applications. (2) Improved nanomaterials targeting: Precise targeting of fluorescent nanomaterials remains challenging due to issues such as off-target binding and rapid clearance. Future advancements should focus on smart responsive nanomaterials that activate fluorescence upon target recognition, as well as multimodal targeting strategies that integrate biological ligands with physicochemical approaches, such as magnetism or pH responsiveness, to improve specificity and stability in complex biological environments. (3) Enhanced signal stability: Fluorescent nanomaterials often face challenges such as photobleaching, quenching, or degradation in biological environments, which can limit their effectiveness in prolonged or real-time applications. To address these issues, further advancements in core-shell structures or surface passivation are essential for enhancing signal durability and ensuring the reliable performance of fluorescent nanomaterials over extended periods and in complex biological conditions. (4) Improved spatial resolution: Achieving high spatial resolution for biomarker localization is challenging due to light scattering and autofluorescence in biological tissues. Future advancements should focus on integrating super-resolution techniques such as STED and SMLM with photostable fluorescent nanomaterials. Additionally, optimizing the signal-to-noise ratio and minimizing background interference will improve imaging contrast and resolution, enabling more accurate biomarker detection in complex biological environments. (5) Scalable production and economic viability: The translation of fluorescent nanomaterials into clinical applications is hindered by challenges in large-scale synthesis, including maintaining consistency in size, morphology, and surface characteristics. Establishing standardized manufacturing protocols and characterization methods is essential for reproducibility and regulatory approval. Additionally, cost-effective synthesis strategies should be developed to enhance economic feasibility and facilitate commercial adoption. (6) Artificial intelligence-driven advancements: Machine Learning (ML) and Deep Learning (DL) accelerate the application of fluorescent nanomaterials in biomarker detection by predicting optimal compositions, refining synthesis conditions, enhancing imaging analysis, and enabling intelligent biosensing. By optimizing fluorescent nanomaterial properties, improving reproducibility, and enabling real-time data processing, ML/DL enhances detection accuracy, stability, and efficiency, driving progress in biomarker detection. In conclusion, addressing these challenges through interdisciplinary approaches will unlock the full potential of fluorescent nanomaterials in biomarker detection and imaging, paving the way for breakthroughs in life sciences, personalized medicine, and disease diagnostics.

CRediT authorship contribution statement

Xuming Sun: Writing – review & editing, Writing – original draft, Conceptualization. **Tong Xiang:** Writing – original draft. **Linyan Xie:** Writing – review & editing, Writing – original draft, Funding acquisition. **Qiongqiong Ren:** Writing – review & editing, Funding acquisition. **Jinlong Chang:** Writing – review & editing. **Wenshuai Jiang:** Writing – review & editing. **Zhen Jin:** Writing – review & editing. **Xiuli Yang:** Writing – review & editing. **Wu Ren:** Writing – review & editing. **Yi Yu:** Writing – review & editing, Funding acquisition.

Funding

This research was funded by the Innovative Research Team (in Science and Technology) in University of Henan Province (24IRTSTHN042) and the Science and Technology Research Project of Henan Province (grand number 242102310037 and 242102310006).

Declaration of competing interest

The authors declare that they have no known competing financial interests or personal relationships that could have appeared to influence the work reported in this paper.

Data availability

No data was used for the research described in the article.

References

[1] F.-S. Ou, S. Michiels, Y. Shyr, A.A. Adjei, A.L. Oberg, Biomarker discovery and validation: statistical considerations, J. Thorac. Oncol. 16 (2021) 537–545, https://doi.org/10.1016/j.jtho.2021.01.1616.

[2] D. Sim, M.C. Brothers, J.M. Slocik, A.E. Islam, B. Maruyama, C.C. Grigsby, R. R. Naik, S.S. Kim, Biomarkers and detection platforms for human health and performance monitoring: a review,, Adv. Sci. 9 (2022) 2104426, https://doi.org/10.1002/advs.202104426.

[3] J. Therriault, T.A. Pascoal, F.Z. Lussier, C. Tissot, M. Chamoun, G. Bezgin, S. Servaes, A.L. Benedet, N.J. Ashton, T.K. Karikari, J. Lantero-Rodriguez, P. Kunach, Y.-T. Wang, J. Fernandez-Arias, G. Massarweh, P. Vitali, J.-P. Soucy, P. Saha-Chaudhuri, K. Blennow, H. Zetterberg, S. Gauthier, P. Rosa-Neto, Biomarker modeling of Alzheimer's disease using PET-based Braak staging, Nat. Aging 2 (2022) 526–535, https://doi.org/10.1038/s43587-022-00204-0.

[4] T. Sahare, B.N. Sahoo, S. Jaiswal, S. Rana, A. Joshi, An account of the current status of point-of-care lateral flow tests for kidney biomarker detection, Analyst 149 (2024) 4811–4829, https://doi.org/10.1039/D4AN00806E.

[5] R. Manikandan, H.-G. Jang, C.-S. Kim, J.-H. Yoon, J. Lee, H.-j. Paik, S.-C. Chang, Nano-engineered paper-based electrochemical biosensors: versatile diagnostic tools for biomarker detection, Coord. Chem. Rev. 523 (2025) 216261, https://doi.org/10.1016/j.ccr.2024.216261.

[6] X. Sun, M. Zhang, L. Xie, Q. Ren, J. Chang, W. Jiang, Material-enhanced biosensors for cancer biomarkers detection, Microchem. J. 194 (2023) 109298, https://doi.org/10.1016/j.microc.2023.109298.

[7] P. Samadi Pakchin, F. Fathi, H. Samadi, K. Adibkia, Recent advances in receptor-based optical biosensors for the detection of multiplex biomarkers, Talanta 281 (2025) 126852, https://doi.org/10.1016/j.talanta.2024.126852.

[8] L. Shen, Y. Chen, L. Hu, C. Zhang, L. Liu, L. Bao, J. Ma, H. Wang, X. Xiao, L. Wu, S. Chen, Development of a highly sensitive, visual platform for the detection of cadmium in actual wastewater based on evolved whole-cell biosensors, ACS Sens. 9 (2024) 654–661, https://doi.org/10.1021/acssensors.3c01811.

[9] L. Wang, Y. Ji, Y. Chen, S. Zheng, F. Wang, C. Li, Recent research progress of fluorescence biosensors based on carbon dots in early diagnosis of diseases, Trends Anal. Chem. 180 (2024) 117962, https://doi.org/10.1016/j.trac.2024.117962.

[10] Y.-T. Liu, Q.-Q. Zhang, S.-Y. Yao, H.-W. Cui, Y.-L. Zou, L.-X. Zhao, Dual-recognition "turn-off-on" fluorescent Biosensor triphenylamine-based continuous detection of copper ion and glyphosate applicated in environment and living system, J. Hazard Mater. 477 (2024) 135216, https://doi.org/10.1016/j.jhazmat.2024.135216.

[11] D. Qian, J. Zhang, Q. Tan, Y. Zhang, Q. Xu, J. Li, H. Li, Localized bicirculating DNAzyme self-feedback amplification strategy for ultra-sensitive fluorescence biosensing of MicroRNA, Anal. Chem. (2025), https://doi.org/10.1021/acs.analchem.4c04417.

[12] J. Huang, S. Xian, Y. Liu, X. Chen, K. Pu, H. Wang, A renally clearable activatable polymeric nanoprobe for early detection of hepatic ischemia-reperfusion injury,, Adv. Mater. 34 (2022) 2201357, https://doi.org/10.1002/adma.202201357.

[13] J. Dolai, R. Ray, S. Ghosh, A. Maity, N.R. Jana, Optical nanomaterials for advanced bioimaging applications, ACS Appl. Opt. Mater. 2 (2024) 1–14, https://doi.org/10.1021/acsaom.3c00357.

[14] W. Li, G.S. Kaminski Schierle, B. Lei, Y. Liu, C.F. Kaminski, Fluorescent nanoparticles for super-resolution imaging, Chem. Rev. 122 (2022) 12495–12543, https://doi.org/10.1021/acs.chemrev.2c00050.

[15] A.B. Chinen, C.M. Guan, J.R. Ferrer, S.N. Barnaby, T.J. Merkel, C.A. Mirkin, Nanoparticle probes for the detection of cancer biomarkers, cells, and tissues by fluorescence, Chem. Rev. 115 (2015) 10530–10574, https://doi.org/10.1021/acs.chemrev.5b00321.

[16] P. Bhatt, D. Kukkar, K.-H. Kim, Fluorescent nanomaterials for the detection of chronic kidney disease, Trends Anal. Chem. 173 (2024) 117572, https://doi.org/10.1016/j.trac.2024.117572.

[17] M.A. Auwalu, S. Li, C. Sun, S. Cheng, Fluorescent nanomaterials for detection and discrimination of amino acids, Adv. NanoBiomed Res. 3 (2023) 2300017, https://doi.org/10.1002/anbr.202300017.

[18] D. Semeniak, D.F. Cruz, A. Chilkoti, M.H. Mikkelsen, Plasmonic fluorescence enhancement in diagnostics for clinical tests at point-of-care: a review of recent technologies,, Adv. Mater. 35 (2023) 2107986, https://doi.org/10.1002/adma.202107986.

[19] K.D. Wegner, N. Hildebrandt, Near infrared quantum dots for biosensing and bioimaging, Trends Anal. Chem. 180 (2024) 117922, https://doi.org/10.1016/j.trac.2024.117922.

[20] W. Gao, H. Zhao, L. Shang, Fluorescent metal nanoclusters for explosive detection: a review, *Trends Analyt. Chem.*, 180 (2024) 117919, https://doi.org/10.1016/j.trac.2024.117919.
[21] H. Zhang, Q. Zhang, N. Li, G. Yang, Z. Cheng, X. Du, L. Sun, W. Wang, B. Li, Advances in the application of carbon dots-based fluorescent probes in disease biomarker detection, Colloids Surf., B 245 (2025) 114360, https://doi.org/10.1016/j.colsurfb.2024.114360.
[22] X. Guo, L. Zhou, X. Liu, G. Tan, F. Yuan, A. Nezamzadeh-Ejhieh, N. Qi, J. Liu, Y. Peng, Fluorescence detection platform of metal-organic frameworks for biomarkers, Colloids Surf., B 229 (2023) 113455, https://doi.org/10.1016/j.colsurfb.2023.113455.
[23] Z. Yang, T. Xu, H. Li, M. She, J. Chen, Z. Wang, S. Zhang, J. Li, Zero-dimensional carbon nanomaterials for fluorescent sensing and imaging, Chem. Rev. 123 (2023) 11047–11136, https://doi.org/10.1021/acs.chemrev.3c00186.
[24] N.N. Atia, P.Y. Khashaba, S.A. El Zohny, A.H. Rageh, Development of an innovative turn-on fluorescent probe for targeted in-vivo detection of nitric oxide in rat brain extracts as a biomarker for migraine disease, Talanta 272 (2024) 125763, https://doi.org/10.1016/j.talanta.2024.125763.
[25] H. Wang, X. Zhang, P. Li, F. Huang, T. Xiu, H. Wang, W. Zhang, W. Zhang, B. Tang, Prediction of early atherosclerotic plaques using a sequence-activated fluorescence probe for the simultaneous detection of γ-glutamyl transpeptidase and hypobromous acid, Angew. Chem. Int. Ed. 63 (2024) e202315861, https://doi.org/10.1002/anie.202315861.
[26] X. Wang, Q. Ding, R.R. Groleau, L. Wu, Y. Mao, F. Che, O. Kotova, E.M. Scanlan, S.E. Lewis, P. Li, B. Tang, T.D. James, T. Gunnlaugsson, Fluorescent probes for disease diagnosis, Chem. Rev. 124 (2024) 7106–7164, https://doi.org/10.1021/acs.chemrev.3c00776.
[27] N. Asadi-Zaki, H. Mardani, H. Roghani-Mamaqani, F. Wang, Stimuli-induced adjustment of spatial distribution of fluorescence resonance energy transfer dyads in smart polymers, Coord. Chem. Rev. 500 (2024) 215518, https://doi.org/10.1016/j.ccr.2023.215518.
[28] Y. Wang, C. Luo, X. Lou, F. Li, Y. Huang, F. Xia, Fluorescent selectivity-enhanced FRET based on 3D photonic crystals for multianalyte sensing, Anal. Chem. 96 (2024) 1630–1639, https://doi.org/10.1021/acs.analchem.3c04547.
[29] J. Chu, A. Ejaz, K.M. Lin, M.R. Joseph, A.E. Coraor, D.A. Drummond, A. H. Squires, Single-molecule fluorescence multiplexing by multi-parameter spectroscopic detection of nanostructured FRET labels, Nat. Nanotechnol. 19 (2024) 1150–1157, https://doi.org/10.1038/s41565-024-01672-8.
[30] R. Wang, G. Xia, W. Zhong, L. Chen, L. Chen, Y. Wang, Y. Min, K. Li, Direct transformation of lignin into fluorescence-switchable graphene quantum dots and their application in ultrasensitive profiling of a physiological oxidant, Green Chem. 21 (2019) 3343–3352, https://doi.org/10.1039/C9GC01012B.
[31] Y. Rout, C. Montanari, E. Pasciucco, R. Misra, B. Carlotti, Tuning the fluorescence and the intramolecular charge transfer of phenothiazine dipolar and quadrupolar derivatives by oxygen functionalization, J. Am. Chem. Soc. 143 (2021) 9933–9943, https://doi.org/10.1021/jacs.1c04173.
[32] J. Luo, Z. Xie, J.W.Y. Lam, L. Cheng, H. Chen, C. Qiu, H.S. Kwok, X. Zhan, Y. Liu, D. Zhu, B.Z. Tang, Aggregation-induced emission of 1-methyl-1,2,3,4,5-pentaphenylsilole, Chem. Commun. (2001) 1740–1741, https://doi.org/10.1039/B105159H.
[33] Y. Duo, Z. Xiang, G. Gao, G. Luo, B.Z. Tang, Biomedical application of aggregation-induced emission luminogen-based fluorescent sensors, Trends Anal. Chem. 167 (2023) 117252, https://doi.org/10.1016/j.trac.2023.117252.
[34] Y. Zhang, Y. Huang, R. Miao, H. Chen, Inorganic-based aggregation-induced luminescent materials: recent advances and perspectives, Small Struct. 4 (2023) 2300157, https://doi.org/10.1002/sstr.202300157.
[35] X.-B. Wang, H.-J. Li, C. Liu, Y.-X. Hu, M.-C. Li, Y.-C. Wu, Simple turn-on fluorescent sensor for discriminating Cys/Hcy and GSH from different fluorescent signals, Anal. Chem. 93 (2021) 2244–2253, https://doi.org/10.1021/acs.analchem.0c04100.
[36] S. Swathy, G.S. Pallam, Girish Kumar, K., Tryptophan capped gold–silver bimetallic nanoclusters-based turn-off fluorescence sensor for the determination of histamine, Talanta 256 (2023) 124321, https://doi.org/10.1016/j.talanta.2023.124321.
[37] S. Deng, X. Men, M. Hu, X. Liang, Y. Dai, Z. Zhan, Z. Huang, H. Chen, Z. Dong, Ratiometric fluorescence sensing NADH using AIE-dots transducers at the point of care, Biosens. Bioelectron. 250 (2024) 116082, https://doi.org/10.1016/j.bios.2024.116082.
[38] X.-B. Wang, H.-J. Li, Q. Li, Y. Ding, C. Hu, Y.-C. Wu, A specifically triggered turn-on fluorescent probe platform and its visual imaging of HClO in cells, arthritis and tumors,, J. Hazard Mater. 427 (2022) 127874, https://doi.org/10.1016/j.jhazmat.2021.127874.
[39] X. Zhang, M. Ding, Y. Mao, X. Huang, X. Xie, L. Song, M. Qiao, J. Zhang, T. Wang, H. Zhu, Z. Li, Y. Wang, M. Dang, A comparative study of "turn-off" mode and "turn-on" mode lateral flow immunoassay for T-2 toxin detection,, Sensor. Actuator. B Chem. 359 (2022) 131545, https://doi.org/10.1016/j.snb.2022.131545.
[40] J. Zhu, M.E. Graziotto, V. Cottam, T. Hawtrey, L.D. Adair, B.G. Trist, N.T. H. Pham, J.R.C. Rouaen, C. Ohno, M. Heisler, O. Vittorio, K.L. Double, E.J. New, Near-infrared ratiometric fluorescent probe for detecting endogenous Cu2+ in the brain, ACS Sens. 9 (2024) 2858–2868, https://doi.org/10.1021/acssensors.3c02549.
[41] Q. Zheng, M.F. Juette, S. Jockusch, M.R. Wasserman, Z. Zhou, R.B. Altman, S. C. Blanchard, Ultra-stable organic fluorophores for single-molecule research, Chem. Soc. Rev. 43 (2014) 1044–1056, https://doi.org/10.1039/C3CS60237K.
[42] G. Jiang, H. Liu, H. Liu, G. Ke, T.-B. Ren, B. Xiong, X.-B. Zhang, L. Yuan, Chemical approaches to optimize the properties of organic fluorophores for imaging and sensing, Angew. Chem. Int. Ed. 63 (2024) e202315217, https://doi.org/10.1002/anie.202315217.
[43] R. Gui, H. Jin, Organic fluorophores-based molecular probes with dual-fluorescence ratiometric responses to in-vitro/in-vivo pH for biosensing, bioimaging and biotherapeutics applications, Talanta 275 (2024) 126171, https://doi.org/10.1016/j.talanta.2024.126171.
[44] P. Reineck, B.C. Gibson, Near-infrared fluorescent nanomaterials for bioimaging and sensing, Adv. Opt. Mater. 5 (2017) 1600446, https://doi.org/10.1002/adom.201600446.
[45] N. Hildebrandt, Biofunctional quantum dots: controlled conjugation for multiplexed biosensors, ACS Nano 5 (2011) 5286–5290, https://doi.org/10.1021/nn2023123.
[46] M.A. Farzin, H. Abdoos, A critical review on quantum dots: from synthesis toward applications in electrochemical biosensors for determination of disease-related biomolecules,, Talanta 224 (2021) 121828, https://doi.org/10.1016/j.talanta.2020.121828.
[47] P. Wu, X.-P. Yan, Doped quantum dots for chemo/biosensing and bioimaging, Chem. Soc. Rev. 42 (2013) 5489–5521, https://doi.org/10.1039/C3CS60017C.
[48] G. Li, J. Yang, Y. Zhang, H. Li, K. Deng, H. Huang, Light-controlled regulation of dual-enzyme properties in YbGd-carbon quantum dots nano-hybrid for advanced biosensing, Anal. Chem. 96 (2024) 13455–13463, https://doi.org/10.1021/acs.analchem.4c01560.
[49] Z.-G. Wang, S.-L. Liu, D.-W. Pang, Quantum dots: a promising fluorescent label for probing virus trafficking,, Acc. Chem. Res. 54 (2021) 2991–3002, https://doi.org/10.1021/acs.accounts.1c00276.
[50] N. Hildebrandt, C.M. Spillmann, W.R. Algar, T. Pons, M.H. Stewart, E. Oh, K. Susumu, S.A. Díaz, J.B. Delehanty, I.L. Medintz, Energy transfer with semiconductor quantum dot bioconjugates: a versatile platform for biosensing, energy harvesting, and other developing applications,, Chem. Rev. 117 (2017) 536–711, https://doi.org/10.1021/acs.chemrev.6b00030.
[51] Z. Moradialvand, L. Parseghian, H.R. Rajabi, Green synthesis of quantum dots: synthetic methods, applications, and toxicity, J. Hazard. Mater. adv. 18 (2025) 100697, https://doi.org/10.1016/j.hazadv.2025.100697.
[52] L. Zhong, W. Liu, Z. Xie, J. Liu, Biomimetic synthesis of RPL14B-based CdSe quantum dots for the detection of heavy metal copper ions, RSC Adv. 14 (2024) 16821–16827, https://doi.org/10.1039/D4RA02022G.
[53] F. Chen, Y. Li, Z. Ma, N. Li, C. Chen, H. Shen, D. Xu, M. Liu, Y. Yuan, L.S. Li, A sensing platform for highly sensitive immunoassay based on metal-enhanced fluorescence of, Sensor. Actuator. B Chem. 408 (2024) 135537, https://doi.org/10.1016/j.snb.2024.135537. CdSe@ZnS.
[54] S. Qian, Z. Wang, Z. Zuo, X. Wang, Q. Wang, X. Yuan, Engineering luminescent metal nanoclusters for sensing applications, Coord. Chem. Rev. 451 (2022) 214268, https://doi.org/10.1016/j.ccr.2021.214268.
[55] Y. Li, M. Zhou, R. Jin, Programmable metal nanoclusters with atomic precision, Adv. Mater. 33 (2021) 2006591, https://doi.org/10.1002/adma.202006591.
[56] S. Zhou, B. Peng, Y. Duan, K. Liu, O. Ikkala, R.H.A. Ras, Bright and photostable fluorescent metal nanocluster supraparticles from invert emulsions, Angew. Chem. Int. Ed. 61 (2022) e202210808, https://doi.org/10.1002/anie.202210808.
[57] T. Chen, H. Lin, Y. Cao, Q. Yao, J. Xie, Interactions of metal nanoclusters with light: fundamentals and applications, Adv. Mater. 34 (2022) 2103918, https://doi.org/10.1002/adma.202103918.
[58] G. Yang, Z. Wang, F. Du, F. Jiang, X. Yuan, J.Y. Ying, Ultrasmall coinage metal nanoclusters as promising theranostic probes for biomedical applications, J. Am. Chem. Soc. 145 (2023) 11879–11898, https://doi.org/10.1021/jacs.3c02880.
[59] L. Ma, J. Wang, Y. Li, D. Liao, W. Zhang, X. Han, S. Man, A ratiometric fluorescent biosensing platform for ultrasensitive detection of Salmonella typhimurium via CRISPR/Cas12a and silver nanoclusters,, J. Hazard Mater. 443 (2023) 130234, https://doi.org/10.1016/j.jhazmat.2022.130234.
[60] H.-H. Deng, X.-Q. Shi, F.-F. Wang, H.-P. Peng, A.-L. Liu, X.-H. Xia, W. Chen, Fabrication of water-soluble, green-emitting gold nanoclusters with a 65% photoluminescence quantum yield via host–guest recognition, Chem. Mater. 29 (2017) 1362–1369, https://doi.org/10.1021/acs.chemmater.6b05141.
[61] J. Qian, Z. Yang, J. Lyu, Q. Yao, J. Xie, Molecular interactions in atomically precise metal nanoclusters, Precis. Chem. 2 (2024) 495–517, https://doi.org/10.1021/prechem.4c00044.
[62] R. Liu, L. Bao, S. Zhang, Z. Wu, J. Zhou, C. Liu, R. Yu, Ratiometric sensors with selective fluorescence enhancement effects based on photonic crystals for the determination of acetylcholinesterase and its inhibitor, J. Mater. Chem. B 8 (2020) 11001–11009, https://doi.org/10.1039/D0TB02197K.
[63] S. Wang, D. Wang, G. Wang, M. Zhang, Y. Sun, J. Ding, Antibacterial carbon dots, Mater. Today Bio 30 (2025) 101383, https://doi.org/10.1016/j.mtbio.2024.101383.
[64] B. Wang, H. Cai, G.I.N. Waterhouse, X. Qu, B. Yang, S. Lu, Carbon dots in bioimaging, biosensing and therapeutics: a comprehensive review,, Small Sci. 2 (2022) 2200012, https://doi.org/10.1002/smsc.202200012.
[65] C. Ji, Y. Zhou, R.M. Leblanc, Z. Peng, Recent developments of carbon dots in biosensing: a review,, ACS Sens. 5 (2020) 2724–2741, https://doi.org/10.1021/acssensors.0c01556.
[66] M.M. Hussain, W.U. Khan, F. Ahmed, Y. Wei, H. Xiong, Recent developments of Red/NIR carbon dots in biosensing, bioimaging, and tumor theranostics, Chem. Eng. J. 465 (2023) 143010, https://doi.org/10.1016/j.cej.2023.143010.
[67] Y. Wang, X. Li, S. Zhao, B. Wang, X. Song, J. Xiao, M. Lan, Synthesis strategies, luminescence mechanisms, and biomedical applications of near-infrared

fluorescent carbon dots, Coord. Chem. Rev. 470 (2022) 214703, https://doi.org/10.1016/j.ccr.2022.214703.
[68] Y. Chen, H. Cui, M. Wang, X. Yang, S. Pang, N and S doped carbon dots as novel probes with fluorescence enhancement for fast and sensitive detection of Cr(VI), Colloids Surf., A 638 (2022) 128164, https://doi.org/10.1016/j.colsurfa.2021.128164.
[69] J. Zhu, H. Chu, J. Shen, C. Wang, Y. Wei, Nitrogen and fluorine co-doped green fluorescence carbon dots as a label-free probe for determination of cytochrome c in serum and temperature sensing, J. Colloid Interface Sci. 586 (2021) 683–691, https://doi.org/10.1016/j.jcis.2020.10.138.
[70] H. Ding, S.-B. Yu, J.-S. Wei, H.-M. Xiong, Full-color light-emitting carbon dots with a surface-state-controlled luminescence mechanism, ACS Nano 10 (2016) 484–491, https://doi.org/10.1021/acsnano.5b05406.
[71] I. Abánades Lázaro, X. Chen, M. Ding, A. Eskandari, D. Fairen-Jimenez, M. Giménez-Marqués, R. Gref, W. Lin, T. Luo, R.S. Forgan, Metal–organic frameworks for biological applications, Nat. Rev. Methods Primers 4 (2024) 42, https://doi.org/10.1038/s43586-024-00320-8.
[72] Y. Zhao, H. Zeng, X.-W. Zhu, W. Lu, D. Li, Metal–organic frameworks as photoluminescent biosensing platforms: mechanisms and applications, Chem. Soc. Rev. 50 (2021) 4484–4513, https://doi.org/10.1039/D0CS00955E.
[73] B. Saboorizadeh, R. Zare-Dorabei, M. Safavi, V. Safarifard, Applications of metal–organic frameworks (MOFs) in drug delivery, biosensing, and therapy: a comprehensive review, Langmuir 40 (2024) 22477–22503, https://doi.org/10.1021/acs.langmuir.4c02795.
[74] J. Wang, D. Li, Y. Ye, Y. Qiu, J. Liu, L. Huang, B. Liang, B. Chen, A fluorescent metal–organic framework for food real-time visual monitoring, Adv. Mater. 33 (2021) 2008020, https://doi.org/10.1002/adma.202008020.
[75] P. Raja Lakshmi, P. Nanjan, S. Kannan, S. Shanmugaraju, Recent advances in luminescent metal–organic frameworks (LMOFs) based fluorescent sensors for antibiotics, Coord. Chem. Rev. 435 (2021) 213793, https://doi.org/10.1016/j.ccr.2021.213793.
[76] Y.-M. Wang, Z.-R. Yang, L. Xiao, X.-B. Yin, Lab-on-MOFs: color-coded multitarget fluorescence detection with white-light emitting metal–organic frameworks under single wavelength excitation, Anal. Chem. 90 (2018) 5758–5763, https://doi.org/10.1021/acs.analchem.8b00086.
[77] L. Liu, J. Dai, Y. Ji, B. Shen, X. Zhang, R.J. Linhardt, Detection of protamine and heparin using a promising metal organic frameworks based fluorescent molecular device BZA-BOD@ZIF-90, Sensor. Actuator. B Chem. 341 (2021) 130006, https://doi.org/10.1016/j.snb.2021.130006.
[78] X.Z. Wang, X.Y. Mao, Z.Q. Zhang, R. Guo, Y.Y. Zhang, N.J. Zhu, K. Wang, P. P. Sun, J.Z. Huo, X.R. Wang, B. Ding, Solvothermal and ultrasonic preparation of two unique cluster-based Lu and Y coordination materials: metal–organic framework-based ratiometric fluorescent biosensor for an ornidazole and ronidazole and sensing platform for a biomarker of amoeba liver abscess, Inorg. Chem. 59 (2020) 2910–2922, https://doi.org/10.1021/acs.inorgchem.9b03272.
[79] X. Liang, H. Wang, J.E. Grice, L. Li, X. Liu, Z.P. Xu, M.S. Roberts, Physiologically based pharmacokinetic model for long-circulating inorganic nanoparticles, Nano Lett. 16 (2016) 939–945, https://doi.org/10.1021/acs.nanolett.5b03854.
[80] C. Su, Y. Liu, R. Li, W. Wu, J.P. Fawcett, J. Gu, Absorption, distribution, metabolism and excretion of the biomaterials used in Nanocarrier drug delivery systems, Adv. Drug Deliv. Rev. 143 (2019) 97–114, https://doi.org/10.1016/j.addr.2019.06.008.
[81] G. Bachler, N. von Goetz, K. Hungerbühler, A physiologically based pharmacokinetic model for ionic silver and silver nanoparticles,, Int. J. Nanomed. 8 (2013) 3365–3382, https://doi.org/10.2147/ijn.s46624.
[82] A. Zhang, K. Meng, Y. Liu, Y. Pan, W. Qu, D. Chen, S. Xie, Absorption, distribution, metabolism, and excretion of nanocarriers in vivo and their influences, Adv. Colloid Interface Sci. 284 (2020) 102261, https://doi.org/10.1016/j.cis.2020.102261.
[83] D. Jiang, Y. Pan, H. Yao, J. Sun, W. Xiong, L. Li, F. Zheng, S. Sun, J.-J. Zhu, Synthesis of renal-clearable multicolor fluorescent silicon nanodots for tumor imaging and in vivo H2O2 profiling, Anal. Chem. 94 (2022) 9074–9080, https://doi.org/10.1021/acs.analchem.2c01308.
[84] P.Y. Li, F. Bearoff, P. Zhu, Z. Fan, Y. Zhu, M. Fan, L. Cort, T. Kambayashi, E. P. Blankenhorn, H. Cheng, PEGylation enables subcutaneously administered nanoparticles to induce antigen-specific immune tolerance, J. Contr. Release 331 (2021) 164–175, https://doi.org/10.1016/j.jconrel.2021.01.013.
[85] M. Xu, Y. Qi, G. Liu, Y. Song, X. Jiang, B. Du, Size-dependent in vivo transport of nanoparticles: implications for delivery, targeting, and clearance, ACS Nano 17 (2023) 20825–20849, https://doi.org/10.1021/acsnano.3c05853.
[86] M. Yu, J. Xu, J. Zheng, Renal clearable luminescent gold nanoparticles: from the bench to the clinic, Angew. Chem. Int. Ed. 58 (2019) 4112–4128, https://doi.org/10.1002/anie.201807847.
[87] V.K. Deb, N. Chauhan, R. Chandra, U. Jain, Recent progression in controlled drug delivery through advanced functional nanomaterials in cancer therapy, BioNanoScience 14 (2024) 2004–2047, https://doi.org/10.1007/s12668-023-01297-6.
[88] H. Xiang, S. He, G. Zhao, M. Zhang, J. Lin, L. Yang, H. Liu, Gold nanocluster-based ratiometric probe with surface structure regulation-triggered sensing of hydrogen sulfide in living organisms, ACS Appl. Mater. Interfaces 15 (2023) 12643–12652, https://doi.org/10.1021/acsami.2c19057.
[89] Y. Meng, Y. Liu, Q. Guo, H. Xu, Y. Jiao, Z. Yang, S. Shuang, C. Dong, Strategy to synthesize dual-emission carbon dots and their application for pH variation and hydrogen sulfide sensing and bioimaging, Spectrochim. Acta Mol. Biomol. Spectrosc. 293 (2023) 122483, https://doi.org/10.1016/j.saa.2023.122483.
[90] Y. Ma, L. Liu, Z. Ye, L. Xu, Y. Li, S. Liu, G. Song, X.-B. Zhang, Engineering of cyanine-based nanoplatform with tunable response toward reactive species for ratiometric NIR-II fluorescent imaging in mice, Sci. Bull. 68 (2023) 2382–2390, https://doi.org/10.1016/j.scib.2023.08.041.
[91] A. Kumar, A. Kumari, P. Mukherjee, T. Saikia, K. Pal, S.K. Sahu, A design of fluorescence-based sensor for the detection of dopamine via FRET as well as live cell imaging, Microchem. J. 159 (2020) 105590, https://doi.org/10.1016/j.microc.2020.105590.
[92] L. Pan, F. Yang, S. Xu, D. Lin, C. Jiang, Fluorescence sensing probe based on functionalized mesoporous MOFs for non-invasive and detection of dopamine in human fluids, Talanta 278 (2024) 126356, https://doi.org/10.1016/j.talanta.2024.126356.
[93] X. Sun, P. Lei, X. Zhang, Q. Wang, B. Li, S. Shuang, C. Dong, The g-C3N4/BSA@MnO2 nanocomposites fluorescent off-on probe for detection and imaging of ascorbic acid in living cells,, Mater. Today Chem. 33 (2023) 101656, https://doi.org/10.1016/j.mtchem.2023.101656.
[94] Z. Yang, T. Xu, S. Zhang, H. Li, Y. Ji, X. Jia, J. Li, Multifunctional N,S-doped and methionine functionalized carbon dots for on-off-on Fe3+ and ascorbic acid sensing, cell imaging, and fluorescent ink applying, Nano Res. 16 (2023) 5401–5411, https://doi.org/10.1007/s12274-022-5107-7.
[95] S.-J. Chung, K. Hadrick, M. Nafiujjaman, E.H. Apu, M.L. Hill, M. Nurunnabi, C. H. Contag, T. Kim, Targeted biodegradable near-infrared fluorescent nanoparticles for colorectal cancer imaging, ACS Appl. Bio Mater. 7 (2024) 7861–7870, https://doi.org/10.1021/acsabm.4c00072.
[96] Y. Ma, D. Liu, W. Xiao, Y. Ye, L. Zhang, X. Chen, Y. Lv, R. Wu, L. Wang, L.S. Li, A low-cost biotin-streptavidin amplified quantum dot fluorescence immunosensor for enhancing cancer detection and imaging, Microchem. J. 207 (2024) 112275, https://doi.org/10.1016/j.microc.2024.112275.
[97] S. Yektaniroumand Digehsaraei, M. Salouti, B. Amini, S. Mahmazi, M. Kalantari, A. Kazemizadeh, J. Mehrvand, Developing a fluorescence immunosensor for detection of HER2-positive breast cancer based on graphene and magnetic nanoparticles, Microchem. J. 167 (2021) 106300, https://doi.org/10.1016/j.microc.2021.106300.
[98] L. Cong, Y. Tian, Z. Huo, W. Xu, C. Hou, W. Shi, W. Wang, C. Liang, S. Xu, Single-cell VEGF analysis by fluorescence imaging–microfluidic droplet platform: an immunosandwich strategy on the cell surface, Anal. Chem. 94 (2022) 6591–6598, https://doi.org/10.1021/acs.analchem.2c00695.
[99] B. Li, S. Yu, R. Feng, Z. Qian, K. He, G.-J. Mao, Y. Cao, K. Tang, N. Gan, Y.-X. Wu, Dual-mode gold nanocluster-based nanoprobe platform for two-photon fluorescence imaging and fluorescence lifetime imaging of intracellular endogenous miRNA, Anal. Chem. 95 (2023) 14925–14933, https://doi.org/10.1021/acs.analchem.3c02216.
[100] Z. Liu, S. Zhou, D. Zhang, M. Yang, CoOOH nanoflake as supporter of CRISPR-Cas12a system for facilitated imaging of miRNA-21 in cells, Sensor. Actuator. B Chem. 424 (2025) 136897, https://doi.org/10.1016/j.snb.2024.136897.
[101] D. Chang, Z. Zhao, W. Niu, L. Shi, Y. Yang, Iron ion sensing and in vitro and in vivo imaging based on bright blue-fluorescent carbon dots, Spectrochim. Acta Mol. Biomol. Spectrosc. 260 (2021) 119964, https://doi.org/10.1016/j.saa.2021.119964.
[102] N. Ding, R. Liu, B. Zhang, N. Yang, M. Qin, Y. Zhang, Z. Wang, A fluorescent nanoprobe and paper-based nanofiber platform for detection and imaging of Fe3+ in actual samples and living cells, Talanta 271 (2024) 125713, https://doi.org/10.1016/j.talanta.2024.125713.
[103] X.-W. Yu, X. Liu, Y.-W. Jiang, Y.-H. Li, G. Gao, Y.-X. Zhu, F. Lin, F.-G. Wu, Rose bengal-derived ultrabright sulfur-doped carbon dots for fast discrimination between live and dead cells, Anal. Chem. 94 (2022) 4243–4251, https://doi.org/10.1021/acs.analchem.1c04658.
[104] H. Wang, B. Li, Y. Sun, Q. Ma, Y. Feng, Y. Jia, W. Wang, M. Su, X. Liu, B. Shu, J. Zheng, S. Sang, Y. Yan, Y. Wu, Y. Zhang, Q. Gao, P. Li, J. Wang, F. Ma, X. Li, D. Yan, D. Wang, X. Zou, Y. Liao, NIR-II AIE luminogen-based erythrocyte-like nanoparticles with granuloma-targeting and self-oxygenation characteristics for combined phototherapy of tuberculosis, Adv. Mater. 36 (2024) 2406143, https://doi.org/10.1002/adma.202406143.
[105] L. Zhao, Y. Fang, X. Chen, Y. Meng, F. Wang, C. Li, Carbon dot-based fluorescent probe for early diagnosis of pheochromocytoma through identification of circulating tumor cells, Spectrochim. Acta Mol. Biomol. Spectrosc. 310 (2024) 123921, https://doi.org/10.1016/j.saa.2024.123921.
[106] J. Ren, Z. Chen, E. Ma, W. Wang, S. Zheng, H. Wang, Dual-source powered nanomotors coupled with dual-targeting ligands for efficient capture and detection of CTCs in whole blood and in vivo tumor imaging, Colloids Surf., B 231 (2023) 113568, https://doi.org/10.1016/j.colsurfb.2023.113568.
[107] Y. Wu, L.-L. Sun, H.-H. Han, X.-P. He, W. Cao, T.D. James, Selective FRET nano probe based on carbon dots and naphthalimide–isatin for the ratiometric detection of peroxynitrite in drug-induced liver injury, Chem. Sci. 15 (2024) 757–764, https://doi.org/10.1039/D3SC05010F.
[108] S. Wang, X. Zhang, Y. Zhang, K. Zhu, X. Liu, J. Zhang, G. Wang, D. Liu, K. Zhao, X. Wang, J. Chen, J. Song, Activatable nanoprobes for dual-modal NIR-II photoacoustic and fluorescence imaging of hydrogen sulfide in colon cancer, Adv. Opt. Mater. 12 (2024) 2302796, https://doi.org/10.1002/adom.202302796.
[109] Q. Feng, S.-a. Wang, B. Ning, J. Xie, J. Ding, S. Liu, S. Ai, F. Li, X. Wang, W. Guan, Evaluation of the tumor-targeting specific imaging and killing effect of a CEA-targeting nanoparticle in colorectal cancer, Biochem. Biophys. Res. Commun. 719 (2024) 150084, https://doi.org/10.1016/j.bbrc.2024.150084.
[110] Y. Tang, W. Wei, Y. Liu, S. Liu, Fluorescent assay of FEN1 activity with nicking enzyme-assisted signal amplification based on ZIF-8 for imaging in living cells,

Anal. Chem. 93 (2021) 4960–4966, https://doi.org/10.1021/acs.analchem.0c05473.
[111] B. Shen, X. Zhang, J. Dai, Y. Ji, H. Huang, Lysosome targeting metal-organic framework probe LysFP@ZIF-8 for highly sensitive quantification of carboxylesterase 1 and organophosphates in living cells, J. Hazard Mater. 407 (2021) 124342, https://doi.org/10.1016/j.jhazmat.2020.124342.
[112] L. Jiang, H. Cai, W. Zhou, Z. Li, L. Zhang, H. Bi, RNA-targeting carbon dots for live-cell imaging of granule dynamics, Adv. Mater. 35 (2023) 2210776, https://doi.org/10.1002/adma.202210776.
[113] C. Ge, Z. Chen, H. Sun, P. Sun, J. Zhao, Y. Wu, J. Xu, M. Zhou, M. Luan, Visually evaluating drug efficacy in living cells using COF-based fluorescent nanoprobe via CHA amplified detection of miRNA and simultaneous apoptosis imaging, Anal. Chim. Acta 1302 (2024) 342502, https://doi.org/10.1016/j.aca.2024.342502.
[114] L. Sun, Y. Huang, C. Ji, C.A. Grimes, Q. Cai, NIR-II multiplexed fluorescence imaging of bacteria based on excitation-selective lanthanide-doped core-shell nanoparticles, Sensor. Actuator. B Chem. 384 (2023) 133669, https://doi.org/10.1016/j.snb.2023.133669.
[115] N. Ma, Y. Liu, D. Chen, C. Wu, Z. Meng, In vivo imaging of exosomes labeled with NIR-II polymer dots in liver-injured mice, Biomacromolecules 23 (2022) 4825–4833, https://doi.org/10.1021/acs.biomac.2c01005.